D2.7. Final WP2 scientific report

WP2 – Green and Renewable distributed electric energy generation and storing

Author: Warsaw University of Technology (WUT)

March 2026

SMARTGYSUM project has been funded by the European Commission's Horizon 2020 Programme

SMARTGYSUM project has been funded by the European Commission's Horizon 2020 Programme

SMARTGYsum has been funded by the European Union's Horizon 2020 Programme under the Grant Agreement GA 955614

Versions:

Version No.	Person in charge	Institution (acronym)	Date	Comments
1	Oleksandr Velihorskyi	CNUT	03.03.2026	First template of the deliverable report
2	Radek Kot	WUT	14.03.2026	Report consolidation based on individual contributions of Jamil Hassan, Ayesha Aslam, Luis Ignacio Martínez Caballero, Anas Abdullah Alvi, Shuyu Ou
3	Mariusz Malinowski	WUT	17.03.2026	Review of the report
4	Radek Kot	WUT	23.03.2026	Final edits
5	Oleksandr Velihorskyi	CNUT	30.03.2026	First template of the deliverable report
6	Enrique Romero	TUT	30.03.2026	Approval and PDF creation for uploading

SMARTGYSUM project has been funded by the European Commission's Horizon 2020 Programme

Technical References:

Project Acronym	**SmartGYsum**
Project Title	Research and Training Network for Smart and Green Energy Systems and Business Models
Project Coordinator (PC)	Enrique Romero (eromero@unex.es) Universidad de Extremadura (UEX)
Project Duration	1 October 2021 – 31 March 2026

Deliverable No.	D2.7
Dissemination Level	Public
Work Package	WP2 – Green and Renewable distributed electric energy generation and storing
Tasks	
Lead Beneficiary	8 - WUT
Contributing beneficiary (ies)	SEPS, WUT, UEX, AAU
Data due of deliverable	31 March 2026
Actual submission date	30 March 2026

Table of Contents

1. Executive summary 6
1.1. Objectives of the deliverable 6
1.2. Organisation of the deliverable 6
2. General progress of the action 7
2.1. WP2 Objectives and tasks 7
2.2. WP2 – Workpackage progress 7
3. WP2 Tasks results 9
3.1. Task 2.1 – IRP1 "Cooperative Smart Inverters for Green Generation Plants" 9
3.1.1. Introduction 9
3.1.2. Scientific outcomes 9
3.1.3. Contribution to the WP objectives 16
3.1.4. Scientific achievements 23
3.2. Task 2.2 – IRP2 "Development of Power Generators for Smart Buildings with Advanced Power Sharing Capabilities" 26
3.2.1. Introduction 26
3.2.2. Scientific outcomes 26
3.2.3. Contribution to the WP objectives 30
3.2.4. Scientific achievements 30
3.3. Task 2.3 – IRP3 "Virtual Power Plant for operation, both isolated and connected" 31
3.3.1. Introduction 31
3.3.2. Scientific outcomes 31
3.3.3. Contribution to the WP objectives 42
3.3.4. Scientific achievements 42
3.4. Task 2.4 – IRP4 "Condition Monitoring for Smart Power Electronic Converter Systems for Distributed Generation" 45
3.4.1. Introduction 45
3.4.2. Scientific outcomes 45
3.4.3. Contribution to the WP objectives 54
3.4.4. Scientific achievements 54
4. Conclusions 56
5. References 56

SMARTGYSUM project has been funded by the European Commission's Horizon 2020 Programme

List of abbreviations

BEN	Beneficiary
Dn	Deliverable (number)
DoA	Description of Action
DS	Doctoral School
ESR	Early Stage Researcher
ETN	European Training Network
GA	Grant Agreement
IRP	Individual Research Project
ITN	Innovative Training Network
MSn	Milestone (number)
MSCA	Marie Sklodowska-Curie Actions
PC	Project Coordinator
REC	Research Ethics Committee
RSC	Recruitment and Secondment Committee
WPn	Work Package (number)

SMARTGYSUM project has been funded by the European Commission's Horizon 2020 Programme

1. Executive summary

This deliverable provides the final report about the scientific activities that were done and the main result obtained related to the implementation of IRPs of ESRs in WP2 of the project.

WP2: Green and Renewable distributed electric energy generation and storing, focused on the research of self-generation and power-sharing infrastructures that ensure a manageable, reliable, and efficient wind and PV generation, as well as storage through distributed systems, enabling connected and isolated energy generation models.

The ESRs associated with the deliverable:

- ESR01 (**Jamil Hassan, Ayesha Aslam**) coordinated by the SENERGY "Products and Services (SEPS) with IRP01: "Cooperative Smart Inverters for Green Generation Plants" with the following goals: To optimize load sharing capabilities; To enable cooperative-based medium-sized photovoltaic (PV) plants to regulate the energy flows in renewable energy communities. To design and validate strategies for operating parallel connected inverters to optimize the overall performance and to deliver ancillary services. To integrate the generation of renewable energy from different members of Renewable Communities while maintaining the integrity, reliability, and security of the system
- ESR02 (**Luis Martínez**) coordinated by the Warsaw University of Technology (WUT) with IRP02: "Development of Power Generators for Smart Buildings with Advanced Power Sharing Capabilities"; with the following goals: To develop generators that enable the diversification of power sources (wind and PV) in smart buildings To optimize the energy generation and the load transfer to storage devices among the different households that conform to Smart Buildings,
- ESR03 (**Anas Abdullah Alvi**) coordinated by the University of Extremadura (UEX)l with IRP03: "Design and validation of Virtual Power Plants for operation, both isolated and connected" with the following goals: To develop a virtual power plant (VPP) to aggregate different sources of renewable Energy able to work isolated and connected with other VPPs; To improve the reliability and efficiency of energy generation Enlargement of the life length of storage devices by optimizing charge and discharge periods.
- ESR04 (**Shuyu Ou**) coordinated by the Aalborg University (AAU) with IRP04 "Condition Monitoring for Smart Power Electronic Converter Systems for Distributed Generation" with the following goals: To design devices and mechanisms for continued monitoring of converter systems; to enhance the resilience of power electronic converters under severe conditions or emergencies by integration of IoT technologies; to research the adaptions needed in converters systems for the requirements of distributed generation .

1.1. Objectives of the deliverable

The objective of the intermediate scientific report is to consolidate and present the results obtained in the corresponding IRPs included in WP2, to show the progress of each individual IRP in WP2 as well as their orientation on the achievement of WP2 objectives.

1.2. Organisation of the deliverable

This deliverable is based on the scientific work carried out by the ESRs under the supervision of the WP2 partners. Their contributions, documented in individual annual reports, have been consolidated into this report, which presents the key results, methodologies, and validations achieved within WP2. Detailed materials such as simulation models, raw experimental data, and source code are not included in this document.

The outcomes presented in this deliverable are consistent with the project timeline and demonstrate that the objectives of WP2, including Deliverables 2.1, 2.2, 2.3, and 2.4, have been achieved.

2. General progress of the action

2.1. WP2 Objectives and tasks

The WP2 has three main scientific objectives:

- To identify and demonstrate new ways of managing electric energy generation by using Renewable Electric Energy Generation (REEG) and Distributed Energy Resources (DER) as agents of a Collaborative Smart Grid (CSG);
- To develop models to describe/predict the behaviour of PV and wind generators and to design the best and safest ways to integrate their generation into existing grids to improve reliability and efficiency;
- To establish power generation patterns and new efficient converters for each technology to determine the best way to coordinate the operation of different and complementary DERs for supplying Smart Buildings or Houses, increasing the Renewable Energy share in the Electric Energy Generation Mix, or providing ancillary services.

The objectives are meant to fulfilled by a proper execution of the following tasks:

- Task 2.1: Cooperative Smart Inverters for Green Generation Plants (SEPS – WUT)
- Task 2.2: Development of Power Generators for Smart Buildings with Advanced Power Sharing Capabilities (WUT – AAU)
- Task 2.3: Virtual Power Plant for operation, both isolated and connected (UEX -TUT)
- Task 2.4: Condition Monitoring for Smart Power Electronic Converter Systems for Distributed Generation (AAU – CAU)

Fifth task of WP (Task 2.5) is an elaboration of partial and final scientific reports (WUT) and is connected more with the project management.

2.2. WP2 – Workpackage progress

ESR	Starting date	General evaluation	Status
1	28/06/2022	Jamil Hassan's contract started on the IRP start date (28 June 2022). His work resulted in four conference publications, and he is currently preparing an additional publication related to the state of the art. He attended two Doctoral Schools: the second SMARTGYsum Doctoral School in November 2022 in Badajoz and the third in July 2023 in Caparica. He completed a first secondment at Warsaw University of Technology in early 2023, where he gained further expertise in control strategies and modulation techniques. Jamil enrolled in the PhD program at the University of Extremadura and successfully completed the first-year coursework. In October 2023, he left the project to take up a position at another institution.	departed from the project
2	01/06/2022	Luis Martínez started his contract on 1 June 2022 and enrolled in the PhD program at WUT in September 2022. He successfully carried out all tasks within IRP02 and completed secondments at Aalborg University and the University of Extremadura. His contract ended in May 2025. He is currently finalizing his PhD, with the defense expected in September or October 2026.	Active in WUT, finalizing his PhD,
3	1/09/2022	Anas Abdullah Alvi started his contract in early August 2022 and subsequently enrolled in the PhD program at UEX. During the reporting period, he successfully carried out all tasks within IRP03 and completed secondments at Warsaw University of Technology and Tallinn University of Technology. During his contract, he published nine conference papers and three journal papers. He is currently finalizing his PhD, with the defense expected in the second half of 2026.	finalizing his PhD,
4	01/08/2022	Shuyu Ou enrolled in the PhD program at AAU at the start of the project. During the reporting period, his research focused on improving reliability by developing a condition monitoring method for IGBT modules in inverters. He obtained experimental results using a Hardware-in-the-Loop setup to validate a model estimating increased on-state resistance based on harmonics in control variables. During his contract, he published four conference papers and three journal papers. He defended his PhD thesis in January 2026	finalized PhD
5	27/06/2024	Ayesha Aslam took over the responsibilities of ESR01 following his departure and quickly became proficient in the scope and tasks of IRP01. During her	finished the contract

		tenure, she completed secondments at Warsaw University of Technology and Universidade NOVA de Lisboa, and published five papers (two conference and three journal). Upon the termination of her contract in September 2025, she decided not to pursue a PhD degree.	

3. WP2 Tasks results

3.1. Task 2.1 – IRP1 "Cooperative Smart Inverters for Green Generation Plants"

3.1.1. Introduction

IRP1 focuses on the development of cooperative smart inverter technologies for green generation plants, emphasizing advanced multilevel topologies, control strategies, and power quality improvements in AC nanogrid and microgrid applications. The research has progressed from theoretical analysis and simulation modeling to supporting hardware preparation.

Scientific outcomes were obtained primarily at **Senergy Products and Services (Badajoz, Spain)**, in collaboration with the **University of Extremadura (Badajoz, Spain)**, utilizing simulation environments such as MATLAB/Simulink and PLECS for inverter design, control tuning, and performance analysis. The previous ESR01 (Jamil Hassan) completed an 8-week secondment at **Politechnika Warszawska in Warsaw**, contributing to early-stage inverter topology studies. Key advancements under the current ESR01 phase also occurred during subsequent secondments, which included 8 weeks at **Politechnika Warszawska in Warsaw, Poland** (focusing on inner control loop tuning and power quality studies, recording of results in conference papers) and 8 weeks at **NOVA School of Science and Technology in Caparica, Portugal** (advancing business model development, related journal paper writing, and completion/submission of work project deliverables).

The work was further advanced through participation and presentations on progress in international doctoral schools, covering inverter topologies, harmonic compensation, and business models. Results have been documented in journal papers, conference submissions, and a book chapter, establishing a strong foundation for cooperative inverter applications in sustainable energy systems.

3.1.2. Scientific outcomes

Previous ESR01 Contributions (Jamil Hassan, 28-06-2022 to 31-10-2023):

The initial phase of IRP1 under previous ESR01 Jamil Hassan established foundational work on three-phase transformerless inverter topologies, with emphasis on neutral point clamped (NPC) designs and comparative analyses aimed at minimizing common mode voltage in photovoltaic applications. This research included performance evaluations under unbalanced conditions, islanding detection, and reviews of multilevel inverter topologies, providing critical groundwork for subsequent cooperative control developments.

Current ESR01 Contributions (Ayesha Aslam, 27-06-2024 to 20-02-2026):

Following the transition, research under current ESR01 shifted focus to advanced control strategies, power quality enhancement, and practical microgrid applications for cooperative smart inverters. Upon arrival in Badajoz, Spain (17 June 2024), initial efforts involved comprehensive literature review, transitioning from the previous PV cooperative topology to a hybrid configuration featuring a 3-phase T-type inverter in parallel with a traditional 2-level voltage source inverter (VSI). Subsequent work progressed through simulation-based design, optimization, secondments, and dissemination, structured as follows:

Review and Analysis of Traditional and Hybrid Multilevel Inverter Topologies

- Comprehensive review and analysis of traditional single-phase/hybrid topologies alongside advanced three-phase transformerless multilevel inverters, building on prior ESR work.
- Participation and project dissemination in Fifth Doctoral School held in Paris, France.
- Following on previous ESR's work, writing and submission of journal paper *Traditional and Hybrid Topologies for Single-/Three-Phase Transformerless Multilevel Inverters (MDPI Electronics)*, detailing comparative assessment of topology performance metrics including efficiency, harmonic distortion and leakage current reduction.

Inner Control Loop Tuning and Power Quality Analysis

- Development of architecture schematic of the revised PV converter topology of a hybrid parallel AC nanogrid system comprising of 2-level voltage source inverter (2L VSI) and 3-level T-type (3L T-type) inverter with separate control systems.

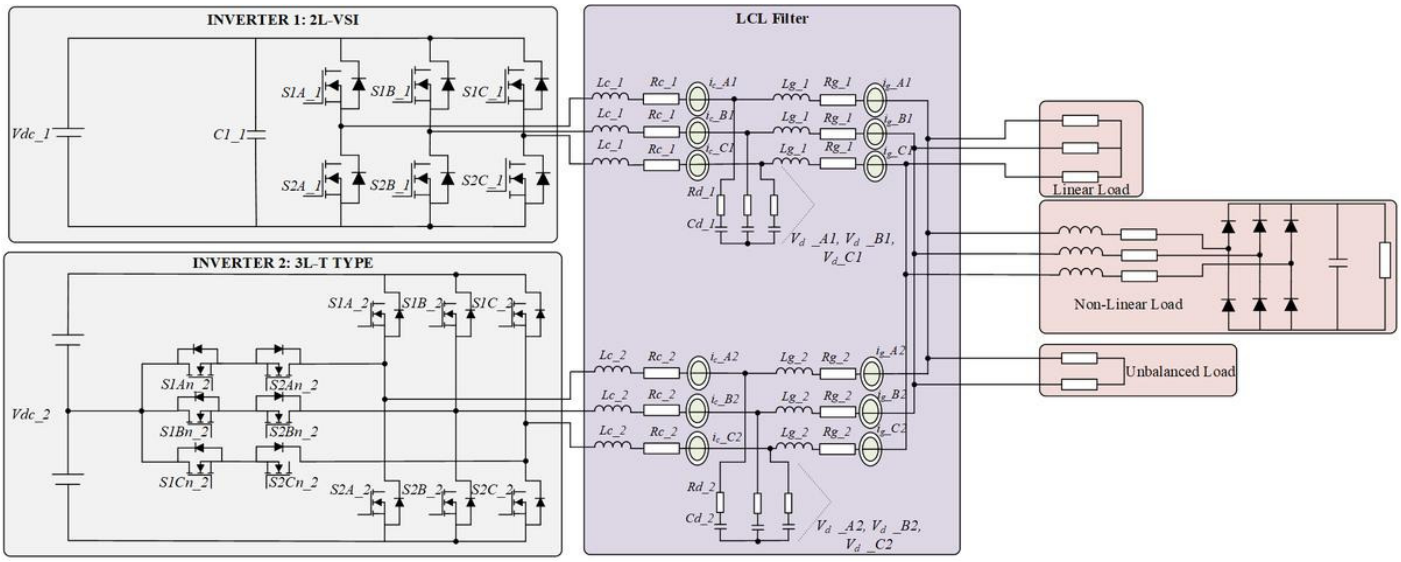

Figure 1 Considered AC nanogrid with parallel hybrid inverter system.

- Simulation and testing of 2L VSI connected with separate control system, LCL filter and linear load run on space vector pulse width modulation (SVPWM) technique in PLECS simulation environment. Control system included the active and reactive power calculation, droop control, virtual impedance loop, outer proportional-resonant PR voltage controller and inner PR current controller. Implementation of PR controllers in discrete time domain using a discretization approach.

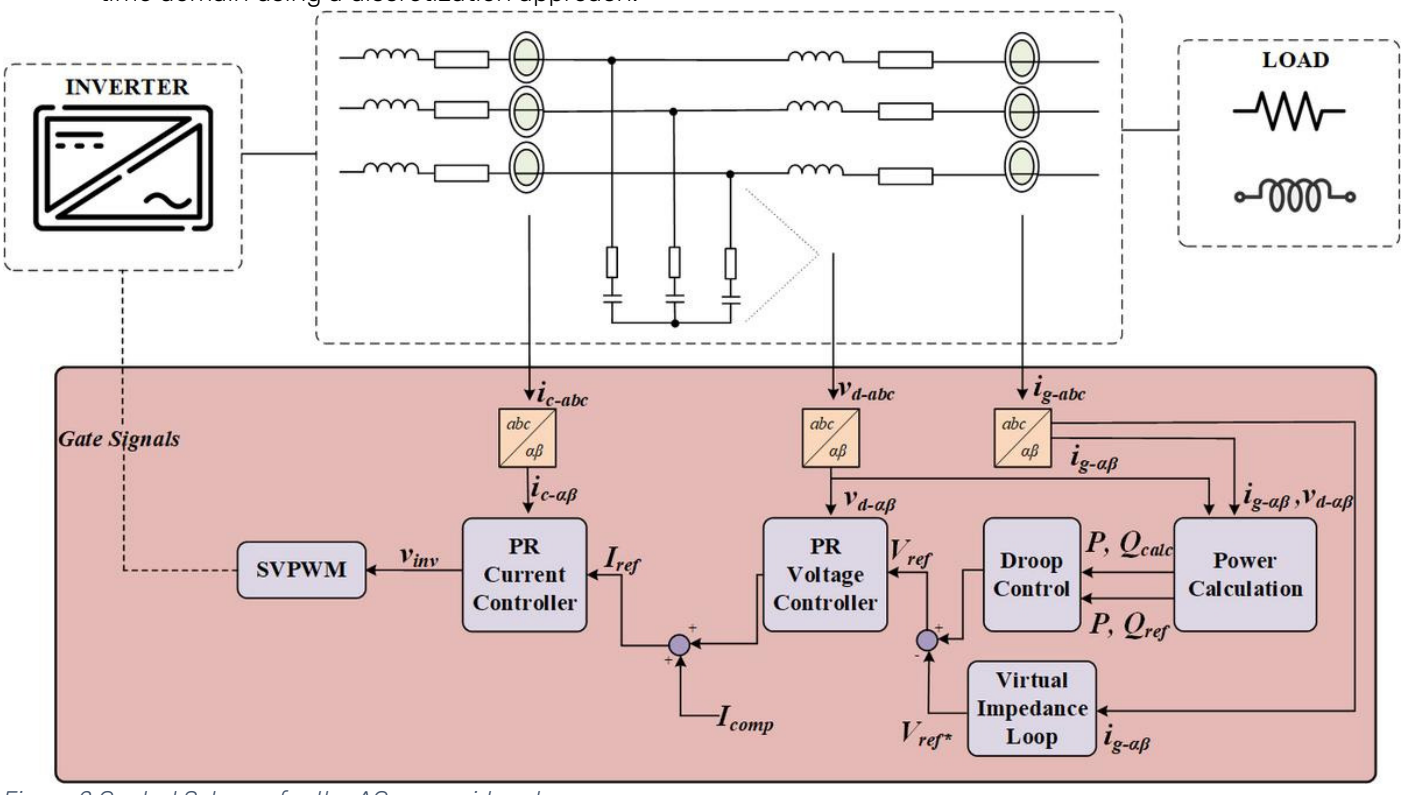

Figure 2 Control Scheme for the AC nanogrid system.

- Simulation and testing of 3L T-type inverter topology connected with separate control system, LCL filter and linear load using SVPWM technique. Control system included the active and reactive power calculation, droop control, virtual impedance loop, outer proportional-resonant PR voltage controller and inner PR current controller. Implementation of PR controllers in discrete time domain using a discretization approach.
- Secondment of 2 months carried out at Warsaw University of Technology, Poland from 23rd October 2024 till 23rd December 2024. The work done during this secondment focused on precise tuning of inner current/voltage control loops using Proportional-Resonant PR controllers, equal power sharing and harmonic compensation in case of non-linear loads. Collaboration with ESR02 in the implementation of discretization

of PR controllers for his system. Co-author collaboration of journal paper, *A Control Strategy for a Standalone PV-Battery System Operating at SoC Boundaries with DC-Link Ripple Management (IEEE Access).*

- Most of the design and tuning studies regarding PR control have been conducted in continuous domain. These tuning algorithms cannot be implemented on digital devices that operate in discrete time domain. Therefore, the goal was to implement and tune the inner control of an islanded AC nanogrid in the discrete time domain. Additionally, the aim was also to integrate this discrete control with the continuous plant to effectively suppress harmonics and voltage unbalances caused by non-linear and unbalanced loads.
  The controller design and tuning scheme is based on requirements related to settling and overshoot time and is further validated by stability analysis for an inverter system connected with LCL filter and load. The algorithm has been implemented using the SISOTOOL tool in MATLAB for the 2L VSI and 3L T-type inverter system.

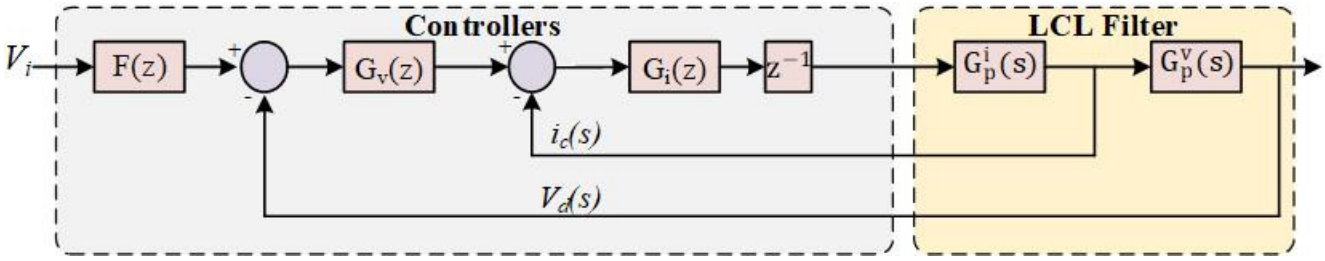

Figure 3 PR controller + plant block diagram used for controller design.

- The controller design has been carried out in discrete time for which the transfer function of the PR controller systems of both inverters was discretized using Tustin with pre-warping method. This method was selected for discretizing the cascaded PR control system due to its superior accuracy in preserving frequency response characteristics, making it particularly suitable for maintaining the stability and performance of resonant controllers in digital implementations. Using the mentioned tuning scheme and considering the design requirements, the proportional and resonant gains for both PR current and voltage controllers were calculated.
- To validate the stability and robustness of the cascaded control system using the obtained controller gains, Bode and Nyquist plots were generated. This stability analysis was conducted in SISOTOOL considering the proportional and resonant gains of the cascaded PR voltage and current controllers respectively. The Bode plot provided insights into the gain and phase margins, providing an assessment of the system response to varying frequencies. The Nyquist diagram further confirmed stability by illustrating the frequency response of the system. It was observed from the Nyquist plot that the system does not encircle the (-1, 0) point, which indicated that the closed-loop system is stable. Together, these plots demonstrated that the controller design meets the stability criteria necessary for reliable operation under varying conditions.
- Writing and submission of conference paper *Tuning and Assessment of Inner Control Loops in an Islanded Nanogrid with Harmonic and Unbalanced Loads (2025 International Aegean Conference on Electrical Machines and Power Electronics (ACEMP) & 2025 International Conference on Optimization of Electrical and Electronic Equipment (OPTIM)),* detailing the design and tuning of PR controllers in discrete domain for an AC nanogrid system followed by its analysis in terms of stability and harmonic mitigation.
- Implementation of power quality analysis on the hybrid AC nanogrid system. The research investigated voltage and current stability, harmonic distortion, and power quality performance under diverse load conditions including linear, non-linear and unbalanced load scenarios.
- Employing the PLECS simulation environment, the study evaluated power quality standards against European electric grid standards, specifically focusing on total harmonic distortion (THD), and voltage imbalance. The aim was to offset unbalanced voltage and suppress harmonics associated with -5th, 7th, -11th and 13th orders. The compensation current is calculated in order to eliminate harmonics in the voltage and negative sequence components. The investigation used an integrated control scheme incorporating multiple second-order generalized integrators (MSOGI), droop control, virtual impedance loops and discretized Proportional-Resonant (PR) controllers. Fourier analysis techniques were implemented to comprehensively assess harmonic characteristics and power quality metrics.

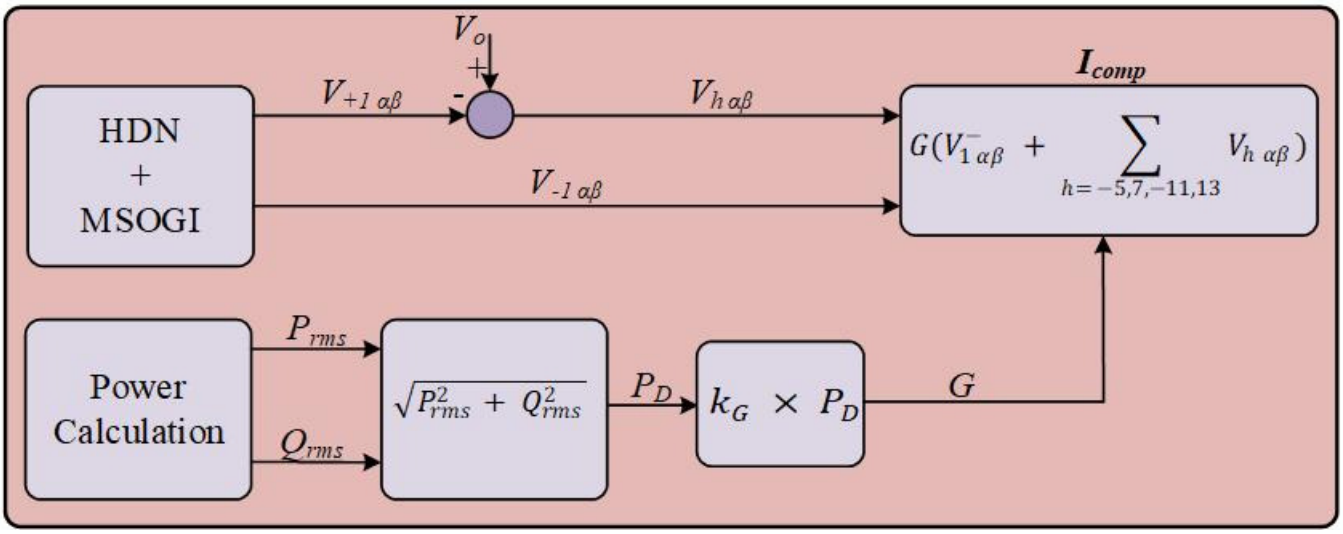

Figure 4 Block diagram of power quality control scheme for generation of compensation current.

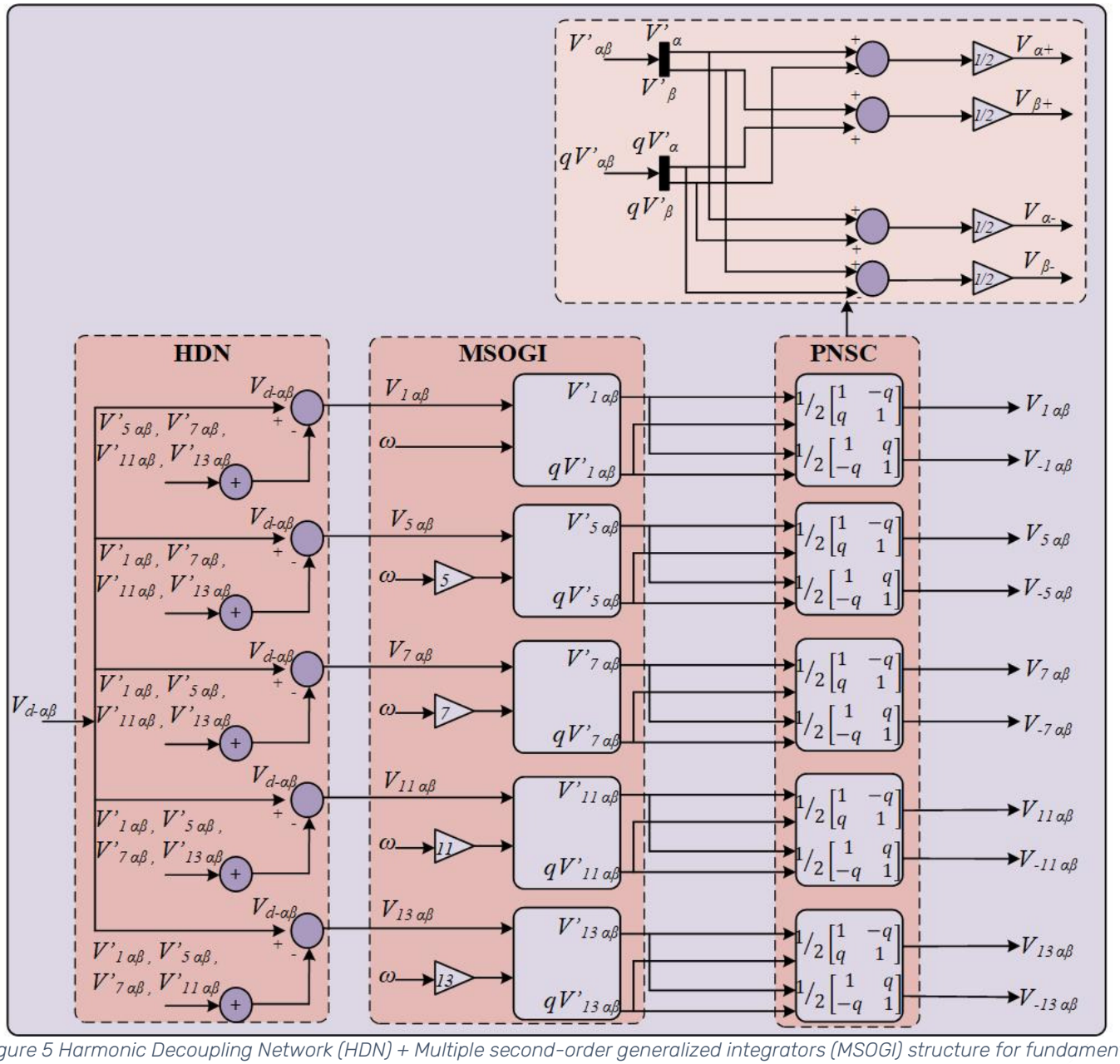

Figure 5 Harmonic Decoupling Network (HDN) + Multiple second-order generalized integrators (MSOGI) structure for fundamental and harmonic extraction.

- Participation and project dissemination in Sixth Doctoral School held in Parnu, Estonia. Development and presentation of initial business model.
- Writing and submission of conference paper, *Power Quality Analysis for Selective Harmonic Compensation in Islanded AC nanogrid (2025 IEEE 19th International Conference on Compatibility, Power Electronics and Power Engineering (CPE-POWERENG))*, detailing a comprehensive power quality analysis investigating voltage and current stability, harmonic distortion, and power quality performance under diverse load conditions.

Droop-Controlled AC Nanogrid and Prototype Development

- Design and development of a grid-forming hybrid parallel AC nanogrid system, focusing on harmonic distortion from non-linear loads which poses a significant challenge to power quality in residential nanogrids, in turn requiring complex control strategies and communication between distributed resources.
- Proposed and designed strategic placement of 2-level voltage source inverter (2L VSI) and 3-level T-type (3L T-type) inverter connected in parallel in an AC hybrid system. The key feature is the connection of the 3L T-type inverter directly with non-linear load. The main idea behind this connection is the dedication of 3L T-type inverter to supply harmonics and reactive current demanded by the non-linear load, through which the system can effectively isolate harmonic pollution at the point of common coupling PCC.

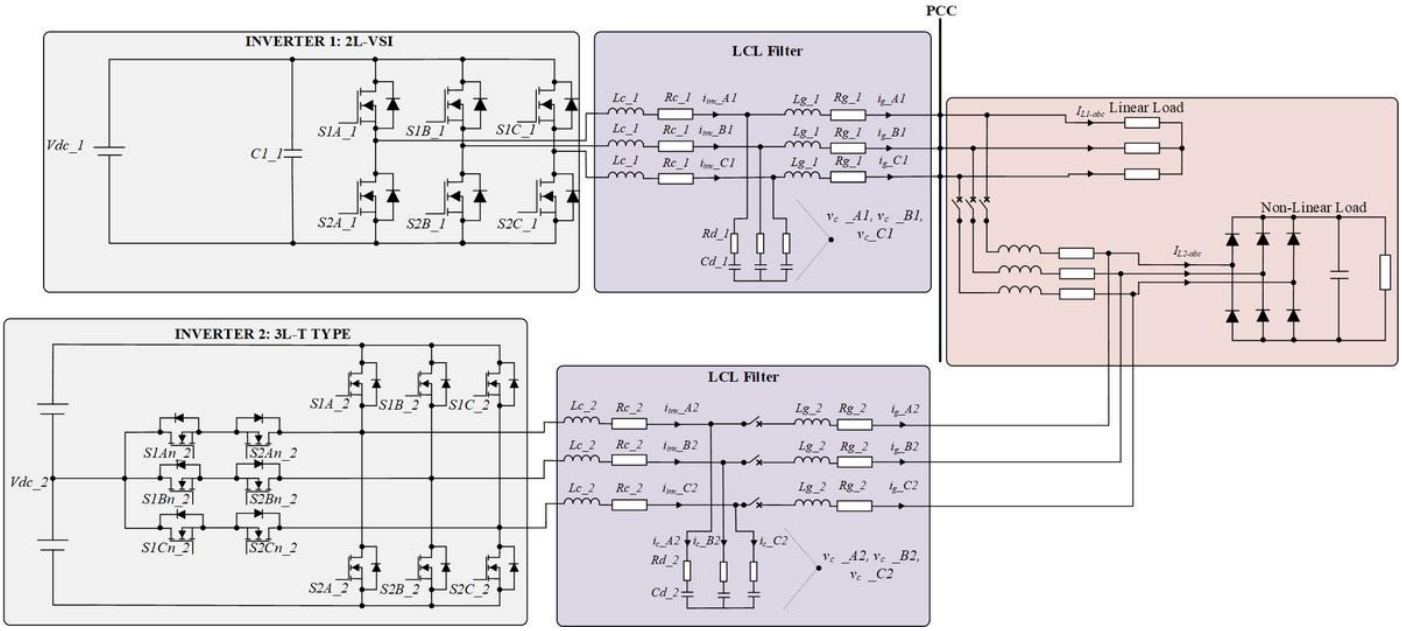

Figure 6 Schematic diagram of the proposed AC nanogrid with parallel hybrid inverter system.

- Design and implementation of a primary droop control, without any secondary or tertiary control layers. This in turn simplified the system and eliminated the need for complex communication infrastructure. The absence of higher-level control layers ensures faster dynamic response and improved system efficiency.
- Implementation of a separate control system for each inverter to enable the strategic placement of the 3L T-type inverter system. Once connected, the reference angle and voltage are determined by the droop equations, which adjust the output based on the measured active and reactive power. This approach ensures a smooth and reliable connection of the 3L T-type inverter to the nanogrid and enables stable, communication-free power sharing with the other inverter.

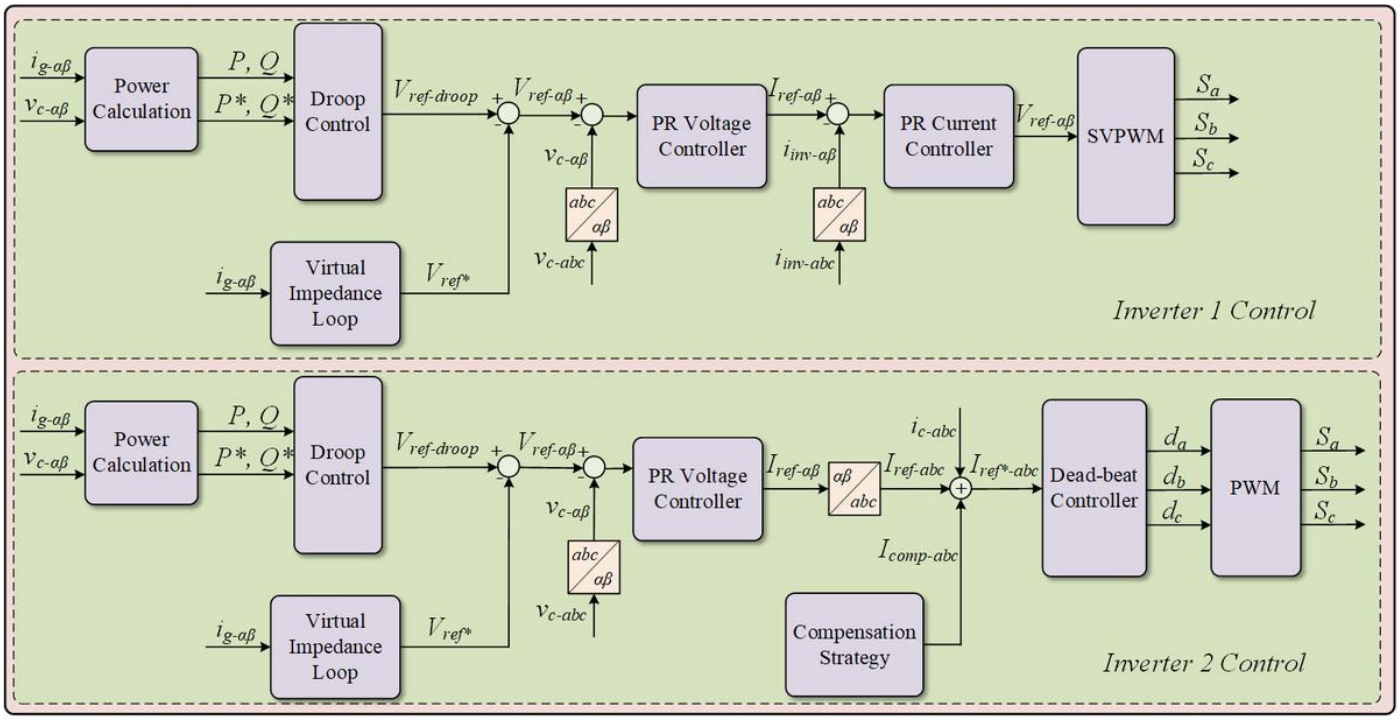

Figure 7 Control scheme of AC nanogrid system.

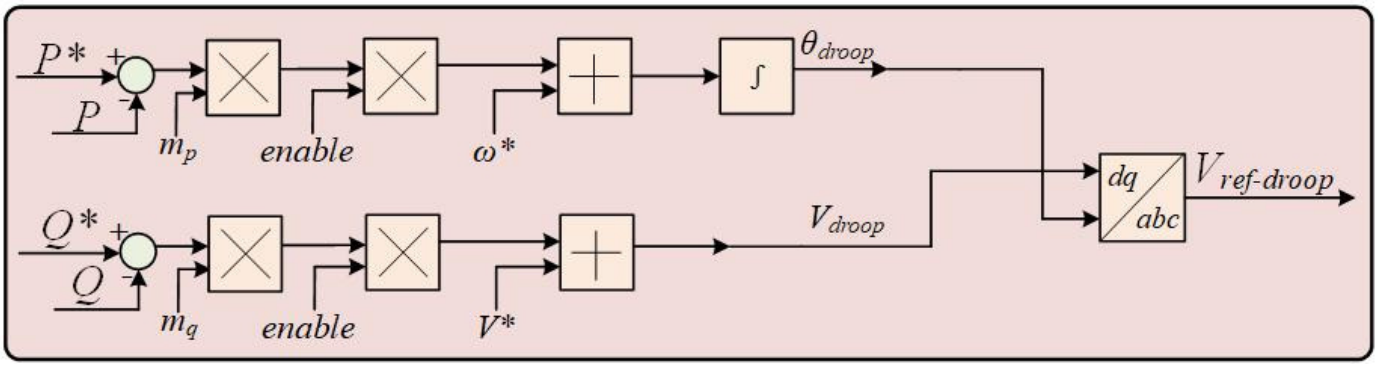

Figure 8 Primary droop control scheme for AC nanogrid system.

- Implementation of a compensation strategy in order to enable the 3L T-type inverter to supply the harmonics and reactive current demanded by non-linear loads. The compensation current is determined as the difference between the measured load current and its fundamental positive-sequence component, and a limiting mechanism ensures the inverter operates within its rated capacity. A synchronous reference frame (SRF) transformation was used to extract the fundamental positive-sequence component from the load current, utilizing the phase angle obtained from the grid voltage. The resulting compensation current targets all harmonic content as well as any unbalanced (negative and zero-sequence) components, enabling the inverter to operate as an effective active power filter.

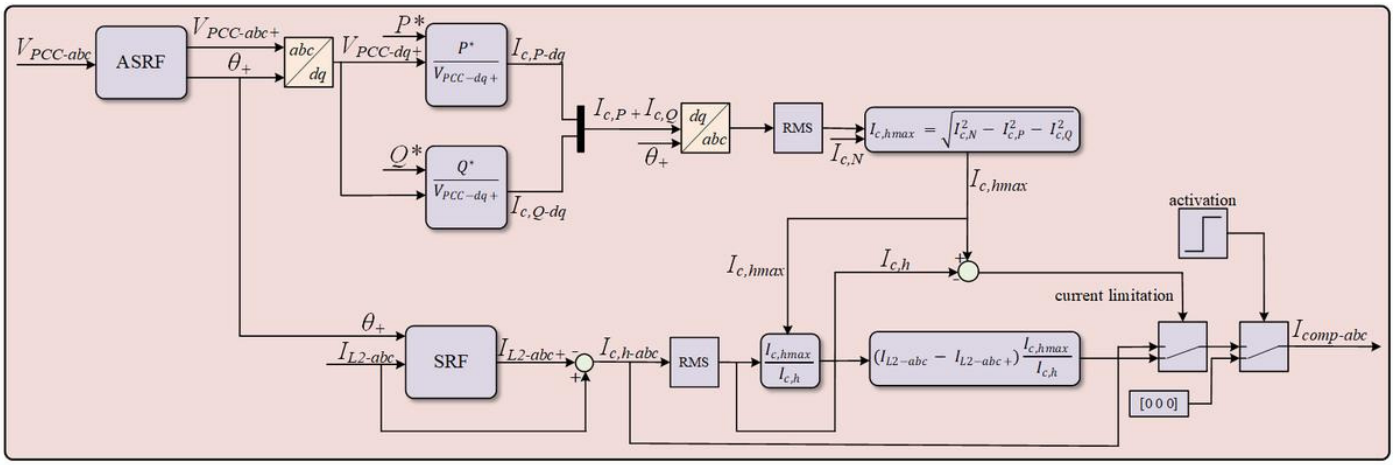

Figure 9 Block diagram of compensation strategy for generation of compensation current.

- Participation and project dissemination in Seventh Doctoral School held in Gdansk, Poland. Participated in and won the business model pitch competition. Documentation of project activities, results and outcomes in a book chapter.
- Writing and submission of journal paper, *A Residential Droop-Controlled AC Nanogrid with Power Quality Enhancement (MDPI Electronics),* focusing on the power quality issue in residential nanogrids due to harmonic distortion from non-linear loads and detailing a parallel hybrid inverter system for an AC nanogrid that enhances power quality using only decentralized droop-based primary control, without the need for secondary control or communication links.
- Prototype development for the proposed hybrid inverter system including separate prototypes for 2L VSI and 3L T-type inverters systems, separate LCL filters and control scheme implementation in RT Box microcontroller for PLECS software.

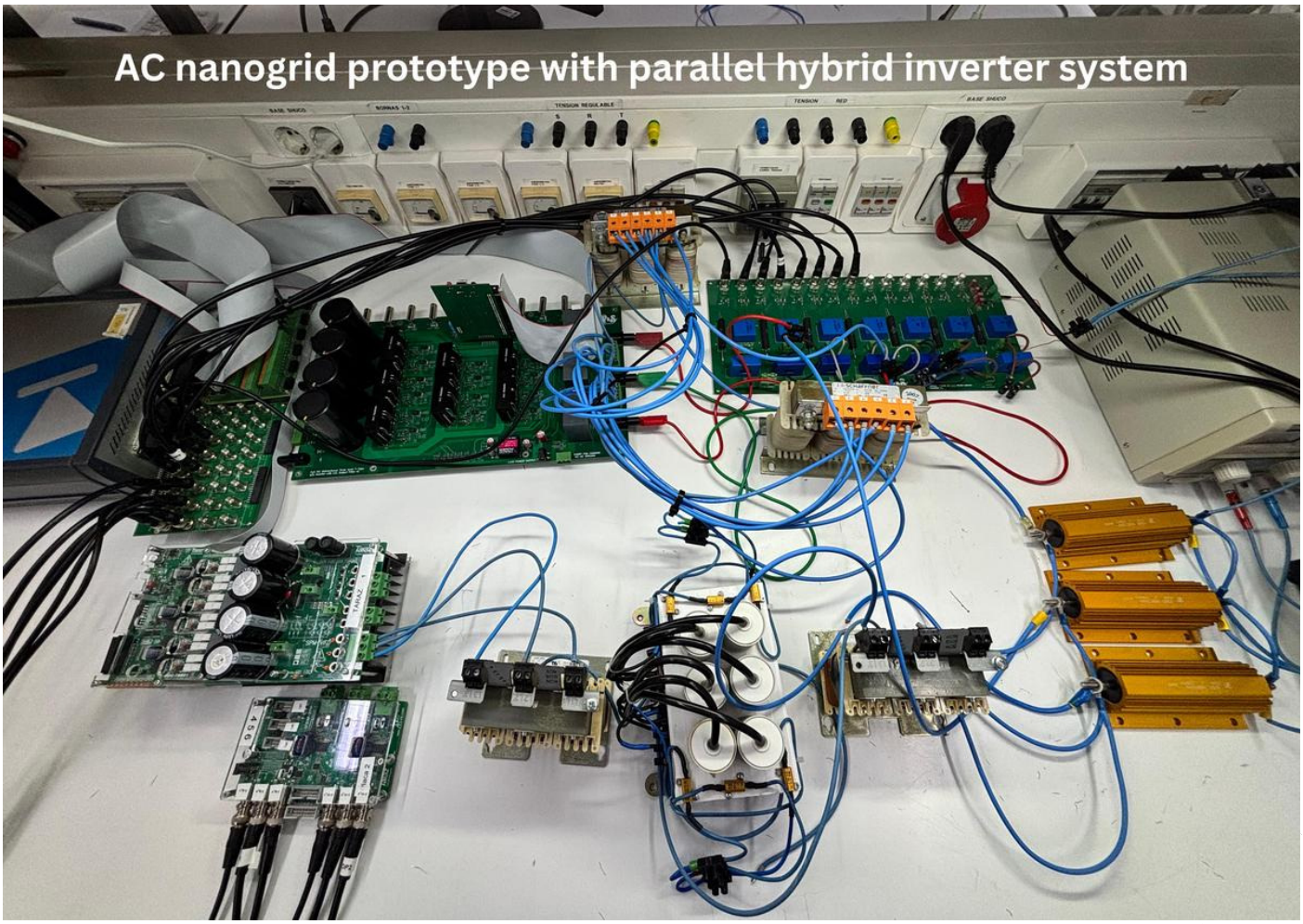

Figure 10 AC nanogrid prototype with parallel hybrid inverter system.

Business Model Integration and Dissemination

- Secondment of 2 months carried out at Nova School of Science and Technology (FCT NOVA) in Caparica, Portugal from 23rd October till 23rd December 2025. The work done during this secondment focused on business model development for cooperative inverter deployment in distributed energy markets.
- Development and evaluation of a commercialization-focused business model for an advanced parallel inverter system integrating both 2L VSI and 3L T-type inverter topologies for distributed energy applications. The business model quantified the influence of design and sourcing decisions on break-even point and potential profitability across different sales and pricing scenarios. The developed business model highlighted how technology selection, production scale, and market dynamics interact to determine viability for early-stage microgrid inverter innovations.
- Writing and submission of journal paper, *Business Model Development for a Hybrid AC Nanogrid with Parallel Inverter Topology: Integrating Engineering and Economic Perspectives (Journal of Modern Power Systems and Clean Energy),* focusing on combining detailed engineering design with systematic bill of materials (BOM) development and market benchmarking to estimate production feasibility and revenue potential. The paper also included discussion on strategic considerations, and practical pathways for the transformation of engineering prototypes into commercially competitive products in the evolving renewable energy sector.

3.1.3. Contribution to the WP objectives

IRP1 directly supports Work Package 2 objectives of developing technologies for efficient management of green/renewable distributed electric energy generation and storing, focusing on sustainability, reliability, power quality and manageability of smart energy systems.

Previous ESR01 Contributions to WP2 Objectives

- **Topology Development for Green Generation:** Three-phase transformerless Neutral Point Clamped (NPC) inverters with common-mode voltage reduction enable efficient PV integration, addressing WP2's sustainability goal through leakage current mitigation and higher conversion efficiency.
- **Grid Reliability under Disturbances:** Performance evaluation of PV plants under unbalanced conditions with islanding detection supports WP2 reliability objectives for distributed generation operating in both grid-connected and islanded modes.
- **Technical Foundation:** Multilevel inverter topology reviews established baseline converter structures suitable for cooperative control, providing groundwork for subsequent power sharing and nanogrid applications.

Current ESR01 Technical Contributions to WP2 Objectives

1. Inner Control Loop Tuning

- **Discretization Design:** The control system design was carried out in discrete time domain for which the transfer function of the cascaded PR controller system was discretized using Tustin with pre-warping method using the SISOTOOL feature in MATLAB. The control system tuning was based on certain requirements related to settling time, rise time and overshoot time. On the basis of these design requirements the resonant and proportional gains for the cascaded control system including PR current and PR voltage controllers were calculated.
- **Discrete-Time Stability:** To validate the stability and robustness of the cascaded control system using the obtained controller gains, Bode and Nyquist plots were generated in SISOTOOL. The Bode plot provided insights into the gain and phase margins, providing an assessment of the system response to varying frequencies. At the resonant frequency (50 Hz or 314 rad/s), the phase response exhibited a sharp increase to 90 degrees which confirmed the stability of the system across its operating range. The Nyquist diagram further confirmed the stability of the closed loop system as the system did not encircle the (-1,0) point.

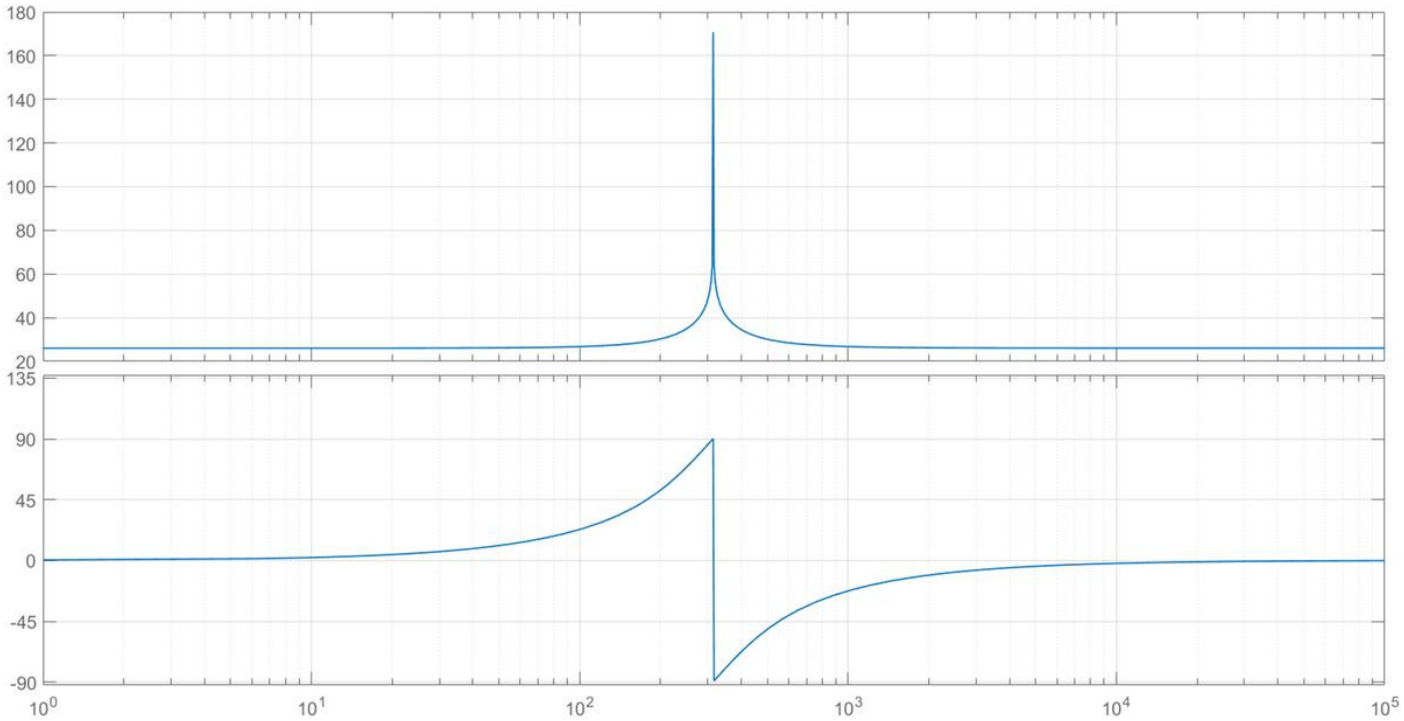

Figure 11 Bode plot for the cascaded control system.

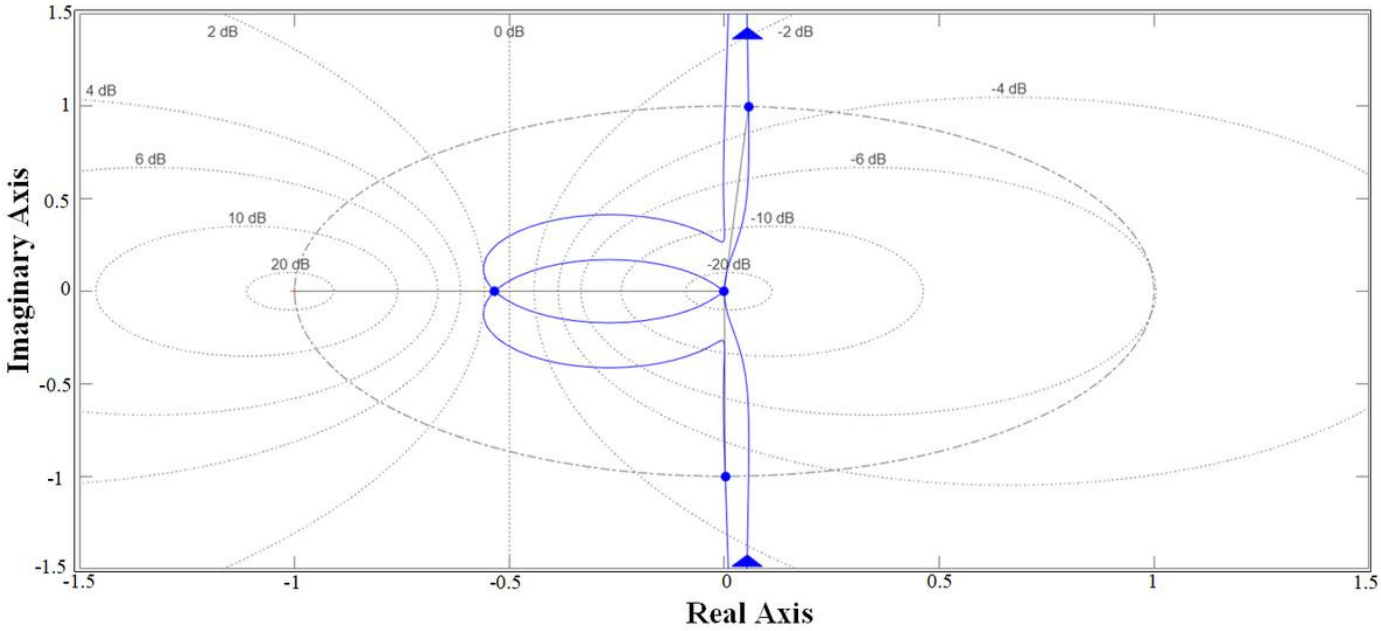

Figure 12 Nyquist diagram for the cascaded control system.

- **WP2 Objectives met:** The discrete-time stability guarantees the implementation on digital devices that operate in discrete time domain for islanded green generation plants. Moreover, the controller tuning process conducted in SISOTOOL optimizes controller performance across diverse LCL parameters, reducing design iteration time. These processes and results comply with the WP2 objective of: **the integration of renewable energy from different members of Renewable Communities while maintaining the integrity, reliability and security of the system**.

2. Power Quality Analysis

- **Load Condition Assessment and Simulation Framework:** The analysis involved the assessment of voltage and current stability, harmonic distortion and power quality performance under diverse load conditions comprising of linear, non-linear and unbalanced loads. The PLECS simulation environment was employed to

conduct a study assessing the power quality indicators against European electric grid standards specifically focusing on total harmonic distortion (THD) and voltage imbalance.

- **Selective Harmonic Compensation Strategy:** The main aim was to offset unbalanced voltage and suppress harmonics associated with -5th, 7th, -11th and 13th orders. After the implementation of power quality scheme, a significant reduction was observed in the harmonic voltages, particularly at the orders mentioned previously. The results validated the effectiveness of the selective harmonic compensation strategy. The calculated compensation current was implemented in order to eliminate harmonics in the voltage and negative sequence components.

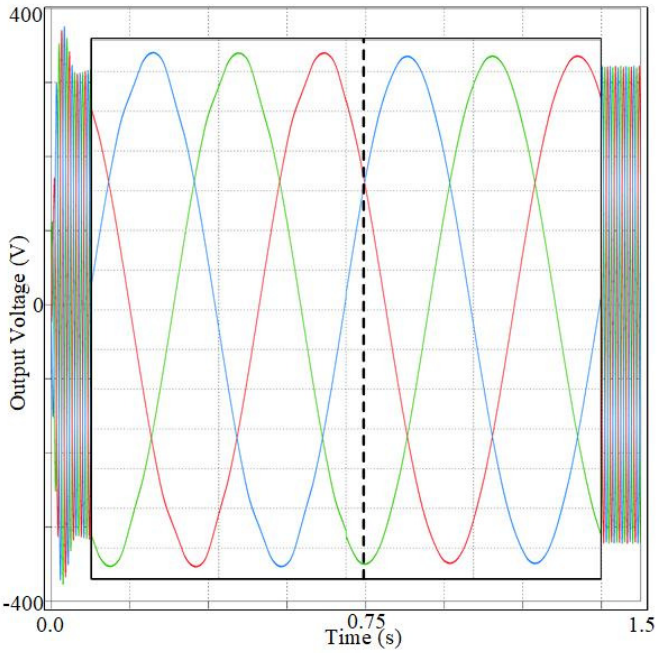

Figure 13 Output voltage of AC nanogrid system before and after inclusion of compensation current.

- **Power Sharing Performance under Compensation:** This selective harmonic compensation and voltage imbalance mitigation, facilitated optimal power sharing between the two inverters in the system. Both inverters (2L VSI and 3L T-type) successfully provided a combined power demand of approximately 5 kW. The data confirmed that both inverters were operating efficiently and contributing equally to the overall power output. The balanced power sharing capability is crucial for maintaining system stability and reliability under varying load conditions.

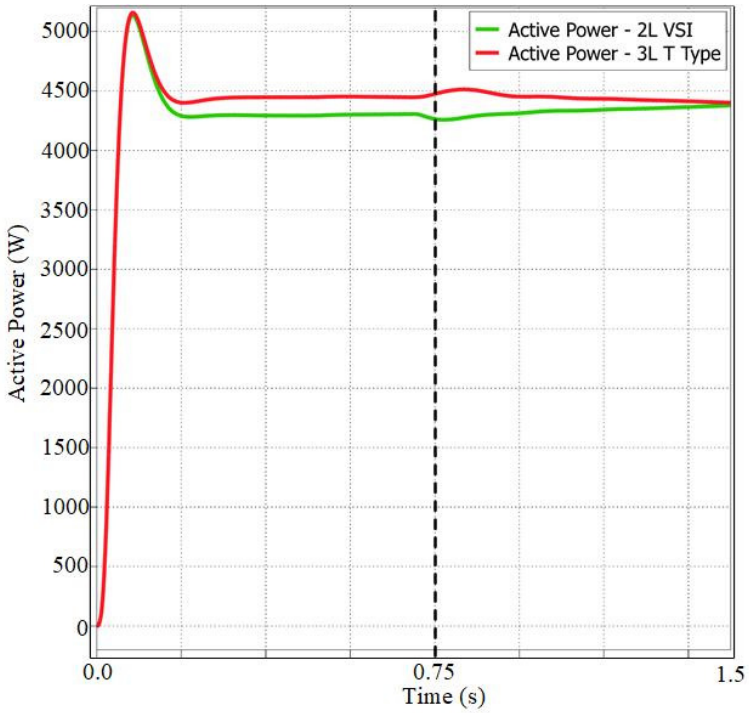

Figure 14 Power sharing performance by both inverters in nanogrid.

- **Fourier Analysis Validation:** Fourier analysis was employed to comprehensively assess the validity of the power quality analysis. Prior to compensation, the Fourier spectrum exhibited notable harmonic components at integral multiples of the fundamental frequency, indicating significant voltage distortion. In contrast, the post-compensation spectrum revealed a marked reduction in the magnitude of the harmonic components, demonstrating the effectiveness of the compensation scheme in mitigating voltage distortion.

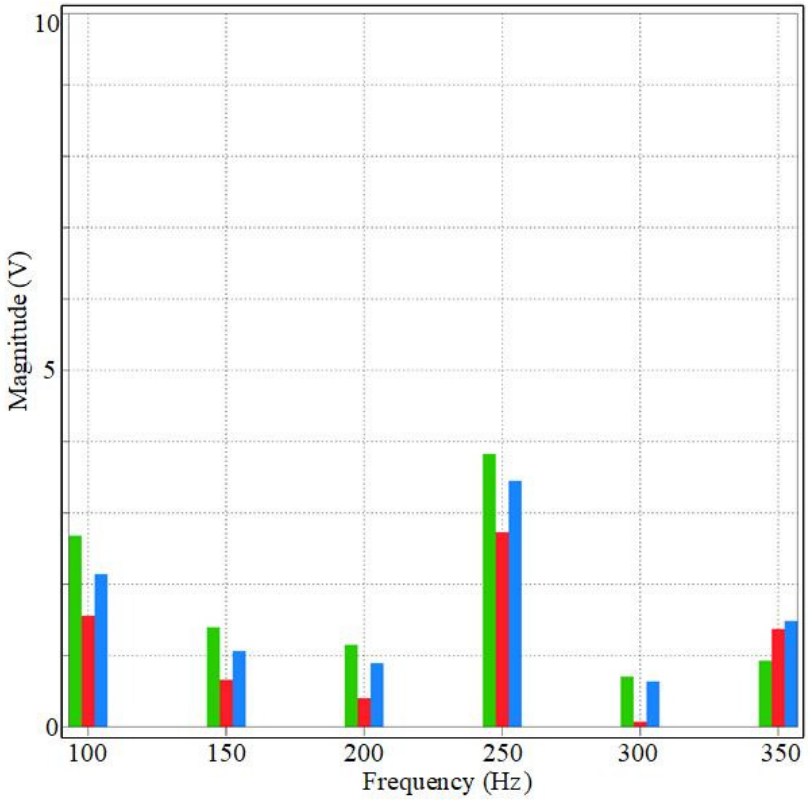

Figure 15 Fourier spectrum of the output voltage before compensation.

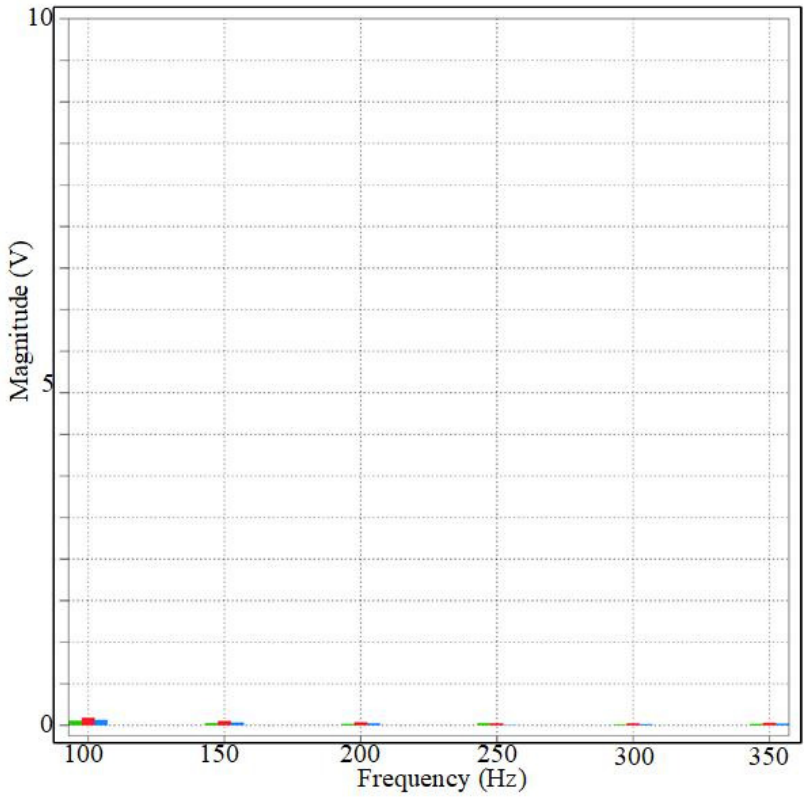

Figure 16 Fourier spectrum of the output voltage after compensation.

- **Power Quality Standards Compliance:** Comprehensive harmonic analysis validated the hybrid AC nanogrid against IEEE 519, EN 50160 and IEC 61000-2-2/12 standards under worst-case grid impedance representative of weak distribution networks. Without compensation current, output voltage THD measured 10.25% with individual harmonics exceeding limits (3rd: 5%, 5th: 6% vs IEEE 519 4-5% limits), while the THD for output current reached 10.8% (3rd: 9.3%, 5th: 5.3%). The selective harmonic compensation scheme targeting 3rd, 5th, 7th and 11th orders reduced voltage THD to 7% (3rd: 4.3%, 5th: 3.75%, 7th: 3.12%, 11th: 2.5%) achieving full EN 50160/IEC compliance for LV networks, and current THD to 3.6% (3rd: 3.33%, 5th: 1.33%, 7th: 0.26%, 11th: 0.06%) meeting IEEE 519 <5% requirements. This validation confirmed the system's capability to deliver grid-quality power from distributed green generation sources despite nonlinear residential loading conditions.
- **WP2 Objectives met:** The MSOGI-based selective harmonic compensation and voltage unbalance mitigation ensure grid-quality power delivery from distributed green generation sources under non-linear and unbalanced residential loads. Furthermore, the comprehensive standards compliance validation maintain power quality during real-world weak grid impedance conditions. These processes and results comply with WP2 objectives of: **developing strategies for operating parallel connected inverters to optimize overall performance, optimizing load sharing capabilities while maintaining integrity and reliability of the system.**

3. Droop-Controlled AC Nanogrid

- **Primary droop control (no secondary/tertiary layers):** Using only primary droop control, with gains selected from realistic inverter ratings and EN 50160 limits, the nanogrid achieved smooth connection of the 3L T-type inverter by enabling through the control system, gradual transition from single inverter to dual inverter operation and balanced active power sharing of 5 kW per inverter for a 10 kW total load without oscillations or circulating currents. The frequency and voltage stay within the allowed deviations defined for low-voltage distribution systems while the droop law continuously adjusts inverter voltage and frequency set-points based on measured active and reactive power, demonstrating that primary control alone is sufficient to ensure stable, communication-free operation in a residential AC nanogrid.
- **Strategic placement of the 3L T-type inverter:** The different stages in the simulation showed that when only the 2L VSI supplied both linear and non-linear loads, the PCC voltage and current became heavily distorted, but once the 3L T-type inverter is connected directly to the non-linear load, it can take over the harmonic and reactive current demand of that branch. After its control was activated, the waveforms at the PCC

reverted to clean sinusoidal voltage and current while the non-linear behaviour was confined to the 3L T-type inverter branch, confirming that the chosen placement effectively isolates harmonic pollution at the load and allows the 2L VSI to focus on the maintaining the fundamental voltage at the PCC.

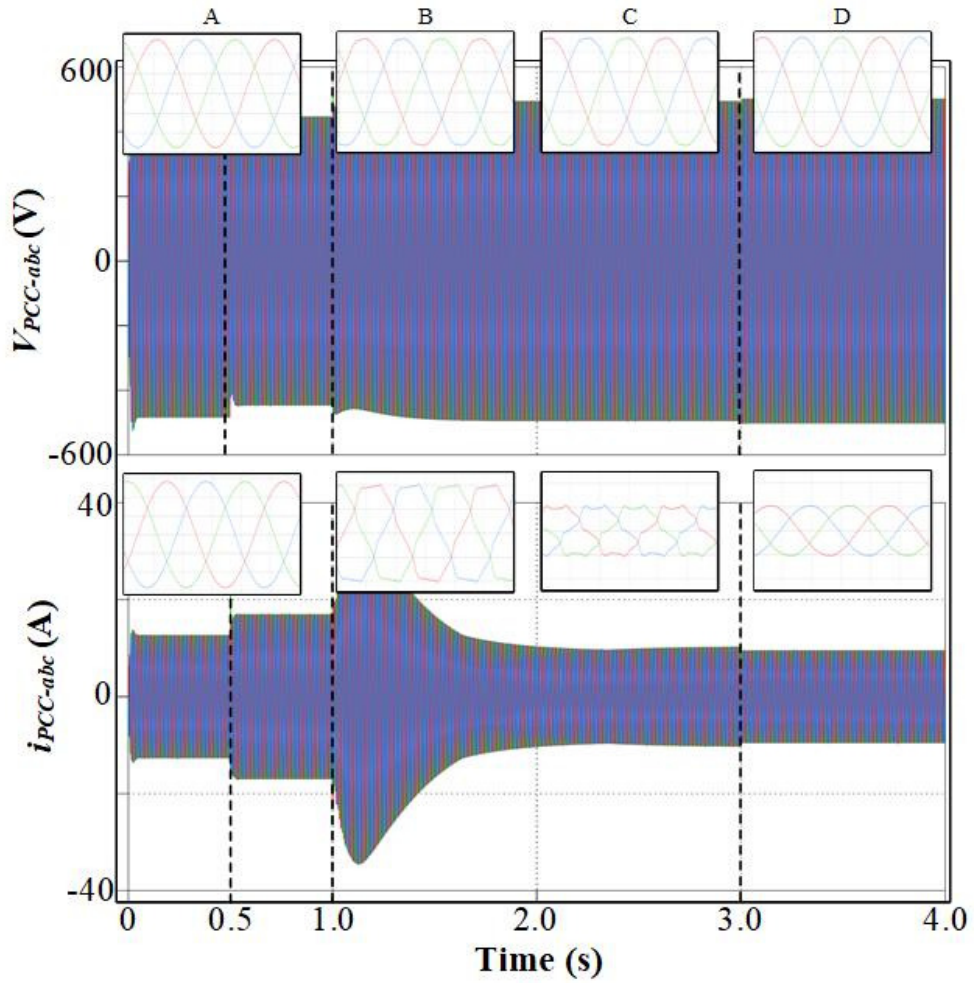

Figure 17 Three-phase PCC voltage and current for the entire simulation period, with Stage A (0-0.5 s), Stage B (0.5-1 s), Stage C (1-3 s), and Stage D (3-4 s).

- **Compensation strategy performance:** When the compensation strategy was disabled, the PCC voltage and current experienced high harmonic distortion (THDv around 15-16% and THDi around 13%), with pronounced low-order harmonics due to the rectifier-type non-linear load. Whereas, after the strategy was enabled, the 3L T-type inverter current became non-sinusoidal to supply the required harmonic and reactive components, reducing the PCC THDv to about 5.3% and THDi to about 2.7%. The individual 3rd, 5th, 7th, 11th and 13th harmonic magnitudes dropped significantly, and the RMS-based limiting of the compensation current ensured that the inverter remained within its rated current, so the system simultaneously restored power quality at the PCC and preserved inverter reliability.

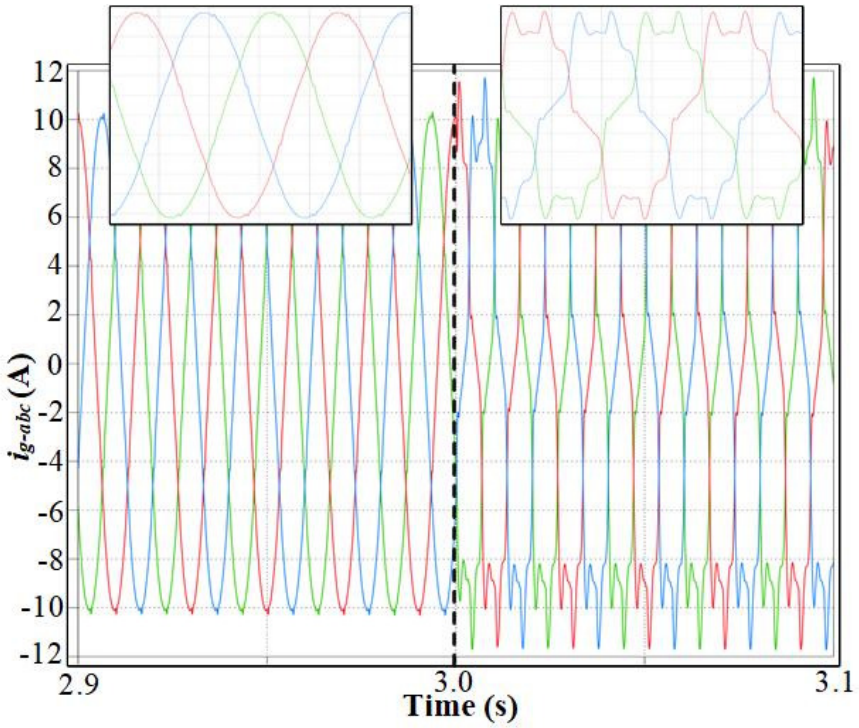

Figure 18 Three-phase output current of 3L T-type inverter before and after compensation strategy implementation.

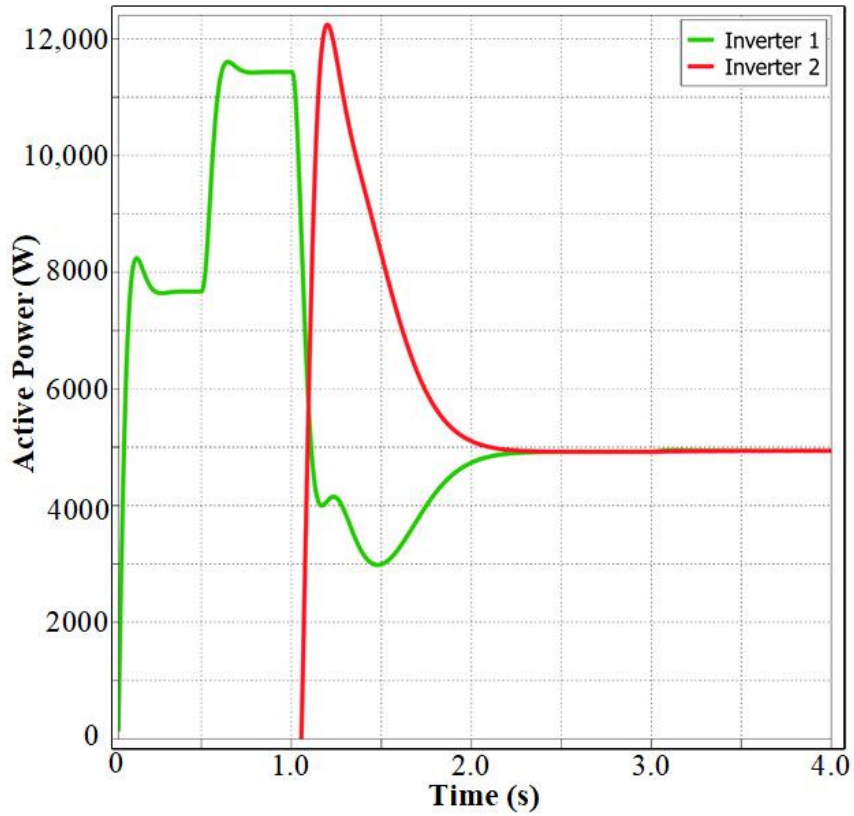

Figure 19 Active power sharing between 2L VSI and 3L T-type inverters.

- **WP2 Objectives met:** The droop-controlled hybrid nanogrid, with strategic inverter placement and targeted compensation, demonstrates that distributed renewable generation can be integrated in a residential setting while maintaining voltage and current within international power-quality limits, ensuring stable power sharing and avoiding reliance on communication-based higher level controls. These results directly support the WP2 objectives of **integrating renewable energy from different members of Renewable Communities while maintaining the integrity, reliability and security of the system by providing a simple, decentralized control**

scheme that guarantees acceptable frequency, voltage and harmonic performance under realistic non-linear conditions.

3.1.4. Scientific achievements

Experimental prototypes

#	Name	Description	Status (designed, assembled, tested)	Photo
1	AC nanogrid prototype with parallel hybrid inverter system	Laboratory-scale AC nanogrid prototype consisting of parallel 2L VSI and 3L T-type inverter units with LCL filters, individual control boards, and measurement interfaces.	Assembled	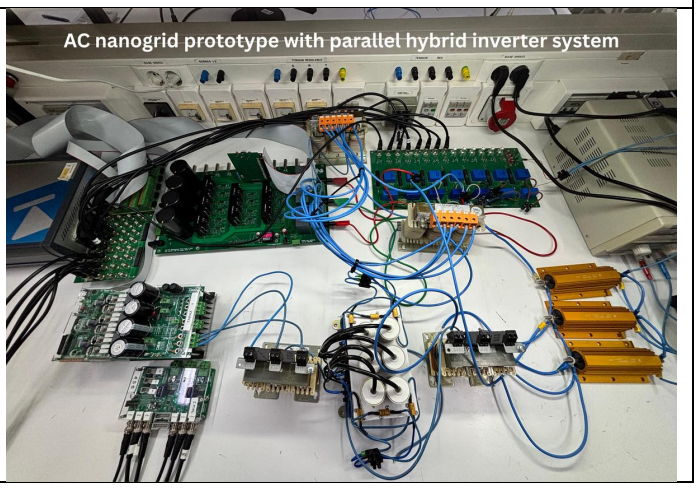

Publication

#	Title, incl. citation information	Type (Conference, journal, book chapter)	Status (Submitted, accepted, published)	DOI
1	An Improved Three-Phase Transformerless Neutral Point Clamped Inverter Topology for Common Mode Voltage Reduction ***Jamil Hassan***, *Victor Minambres-Marcos, Fermin Barrero-Gonzalez, Anas Abdullah Alvi*	Conference – 2023 IEEE 17th International Conference on Compatibility, Power Electronics and Power Engineering (CPE-POWERENG)	Published	10.1109/CPE-POWERENG58103.2023.10227487
2	A Comparative Study of Three-Phase Inverter Topologies for Common Mode Voltage Reduction in Photovoltaic Applications ***Jamil Hassan***, *Victor Minambres-Marcos, Fermin Barrero-Gonzalez, Anas Abdullah Alvi, Mariusz Malinowski, Luis Martinez-Caballero*	Conference - 2023 25th European Conference on Power Electronics and Applications (EPE'23 ECCE Europe)	Published	10.23919/EPE23ECCEEurope58414.2023.10264522
3	An Overview of the Functions of Smart Grids Associated with Virtual Power Plants Including Cybersecurity Measures *Anas Abdullah Alvi, Enrique Romero-Cadaval, Eva González-Romera,* ***Jamil Hassan*** *& Dmitri Vinnikov*	Conference – Doctoral Conference on Computing, Electrical and Industrial Systems	Published	10.1007/978-3-031-36007-7_7

4	Performance Evaluation of a Three-Phase PV Power Plant under Unbalanced Conditions with Islanding Detection Reliability Test *Anas Abdullah Alvi; Enrique Romero-Cadaval; Eva González-Romera; Dmitri Vinnikov;* ***Jamil Hassan***	Conference – 2023 IEEE 17th International Conference on Compatibility, Power Electronics and Power Engineering (CPE-POWERENG)	Published	10.1109/CPE-POWERENG58103.2023.10227391
5	Traditional and Hybrid Topologies for Single-/Three-Phase Transformerless Multilevel Inverters ***Ayesha Wajiha Aslam****, Jamil Hassan, Victor Minambres-Marcos, Ali Gaeed Seger Al-salloomee, Carlos Roncero-Clemente*	Journal – MDPI Electronics	Published	10.3390/electronics13204058
6	Tuning and Assessment of Inner Control Loops in an Islanded Nanogrid with Harmonic and Unbalanced Loads ***Ayesha Wajiha Aslam****, Ali Gaeed Seger Al-Salloomee, Javier Gutiérrez-Escalona, Carlos Roncero-Clemente, Víctor Minambres-Marcos*	Conference – 2025 International Aegean Conference on Electric Machines and Power Electronics (ACEMP) & 2025 International Conference on Optimization of Electrical and Electronic Equipment (OPTIM)	Published	10.1109/OPTIM-ACEMP62776.2025.11075248
7	Power Quality Analysis for Selective Harmonic Compensation in Islanded AC Nanogrid ***Ayesha Wajiha Aslam****, Ali Gaeed Seger Al-Salloomee, Anas Abdullah Alvi, Fermín Barrero-González, Víctor Minambres-Marcos, Carlos Roncero-Clemente*	Conference – 2025 IEEE 19th International Conference on Compatibility, Power Electronics and Power Engineering (CPE-POWERENG)	Published	10.1109/CPE-POWERENG63314.2025.11027243
8	Cooperative Smart Inverters for Green Generation Plants WP2 – Green and Renewable Distributed Electric Generation and Storing ***Ayesha Wajiha Aslam****, Víctor Minambres-Marcos, Carlos Roncero-Clemente*	Book Chapter - SMARTGYsum	Published	ISBN: 978-84-09-81019-2
9	A Residential Droop-Controlled AC Nanogrid with Power Quality Enhancement ***Ayesha Wajiha Aslam****, Víctor Minambres-Marcos, Carlos Roncero-Clemente*	Journal – MDPI Electronics	Published	10.3390/electronics14163306
10	A Control Strategy for a Standalone PV-Battery System Operating at SoC boundaries with DC-Link Ripple Management *Luis Martínez-Caballero,* ***Ayesha Aslam****, Radek Kot,*	Journal – IEEE Access	Published	10.1109/ACCESS.2025.3625405

	Adam Milczarek, Mariusz Malinowski			
11	Business Model Development for a Hybrid AC Nanogrid with Parallel Inverter Topology: Integrating Engineering and Economic Perspectives ***Ayesha Wajiha Aslam**, Víctor Minambres-Marcos*	Journal – Journal of Modern Power Systems and Clean Energy	Submitted	NA

This part has documented the complete progression of IRP1 within Work Package 2 (WP2) of the SMARTGYsum project, from the initial topology-focused work of the previous ESR01 to the subsequent development of control, power quality, nanogrid operation, and business model frameworks under the current ESR01. The combined efforts have provided a fully realised concept for cooperative smart inverters in residential nanogrid environments, supported by validated models, control schemes, and dissemination through various publications.

From a technical standpoint, the project has delivered a hybrid parallel AC nanogrid architecture combining a 2L VSI and 3L T-type inverters, with discretized PR-based inner control loops, virtual impedance, comprehensive compensation strategy and a primary droop control strategy enabling stable, communication-free power sharing. The integration of MSOGI-based harmonic compensation and a strategically placed 3L T-type inverter directly at the non-linear load has been shown to significantly improve power quality, reducing current and voltage distortion to within international grid code limits while maintaining balanced power sharing and respecting inverter ratings.

The work has also demonstrated that advanced control and power quality enhancements can be realized using only primary droop control, without secondary or tertiary control layers or dedicated communication infrastructure, which is especially relevant for cost-sensitive residential nanogrids. The simplification does not compromise performance and enables fast dynamic response, robust operation under non-linear and unbalanced loading while also facilitating future deployment in distributed renewable energy communities.

Beyond the technical results, IRP1 has contributed to the economic objectives of WP2 through the development of a commercialization-oriented business model for the proposed hybrid nanogrid solution. By linking converter design choices, component selection, and control capabilities with cost, scalability, and market viability, the work aligns the technical innovations with realistic pathways for adoption in emerging green energy markets.

Overall, IRP1 presents a coherent and dissemination-supported contribution that advances cooperative smart inverter technology, supports reliable integration of renewable generation at the distribution level, and offers both technical and economic foundations for future deployment within smart and green energy systems and business models.

3.2. Task 2.2 – IRP2 "Development of Power Generators for Smart Buildings with Advanced Power Sharing Capabilities"

3.2.1. Introduction

This section summarizes the work conducted during the development of IRP2: "Development of power generators for Smart Buildings with Advanced Shared Capabilities. The scientific outcomes presented in this report were obtained over a period of 36 months, mainly at the facilities of the Institute of Control and Industrial Electronics of the Warsaw University of Technology, and complemented with research collaborations with the Energy department from Aalborg University, and with the company SynergyPS in Badajoz, Spain, to deliver business models.
The implementation followed a three-stage methodology: state-of-the-art review, design and simulation, and prototype development and validation.

The research contributions include the development of internal controllers, power-sharing for standalone operation, and a novel ancillary service that enables the residential system to provide constant power at the Point of Common Coupling (PCC) for a predefined time, and comparison of energy management techniques. These contributions were validated in simulations and/or experimentally in a laboratory environment using hardware-in-the-loop platforms, the developed prototype, and energy sources emulators such as photovoltaic (PV) arrays, low-voltage distribution network, loads, and batteries.

3.2.2. Scientific outcomes

Critical challenges were addressed from different perspectives, ranging from new proposals for the local controllers of power converters to the comparison of energy management systems in residential applications. To provide sufficient context, the diagram of the system under study is presented in Figure 4. Each power electronic converter is composed of a set of half-bridges: four for the grid-side converter and two for each DC-DC converter. For each half-bridge, two MOSFETS and one gate driver per switching element are used. The grid side converter is a four-leg, three-phase converter connected to an LC filter in the three phases, and an L filter is used for the neutral leg. The filtering stage is followed by an additional breaker that enables the connection with a Chroma 6180. This device emulates the connection of a three-phase low-voltage network under safe operating conditions. Besides, to emulate balanced or unbalanced loads a set of three Chroma 63804 programmable loads are used. The coupling of the DC-AC converter and the DC-DC stage is made by means of a bank of electrolytic capacitors labeled as C_{dc}.

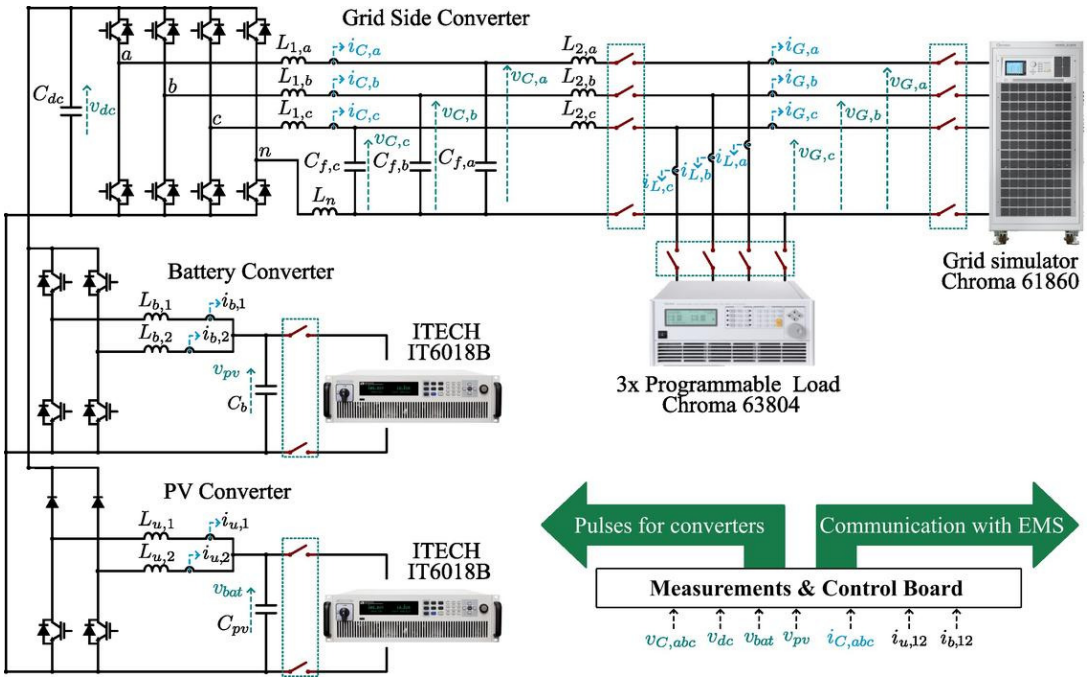

Figure 4. Experimental prototype diagram.

A bidirectional converter is used for the energy conversion stage of the battery system. At the input of this converter one inductor per switching leg is used, and the inductors are connected to a small capacitor in parallel with an ITECH IT6018B bidirectional source. This device is utilized to emulate the behavior of a real battery, allowing to simulate different technologies, power levels and dynamic conditions. A detailed discussion of each resulting contribution is presented below.

Single current controller for different operation modes of the PV converter

The boost converter used in PV applications suffers from two different conduction modes, discontinuous and continuous, depending on the output power and the size of passive components. Although alternatives to this issue have been proposed, their drawbacks include additional or switching controllers, dependence on the operating point during the controller tuning stage, and a lack of experimental validation of a seamless transition between both operating modes. Therefore, based on the well-known averaging technique, a large-signal model valid for any conduction mode was obtained. This has the advantage of requiring only one controller and makes the tuning procedure valid regardless of the conduction mode. The validation was conducted through simulations and compared in an experimental setup with the power conversion stage of the PV system.

Results of both simulations and experiments are shown in Figure 5. The inductor currents of both converter legs are shown, and it is worth noting that the simulation and experimental results are plotted on the same graph, showing a clear overlap between the two, which demonstrates the accuracy of the model in relation to the experimental setup.

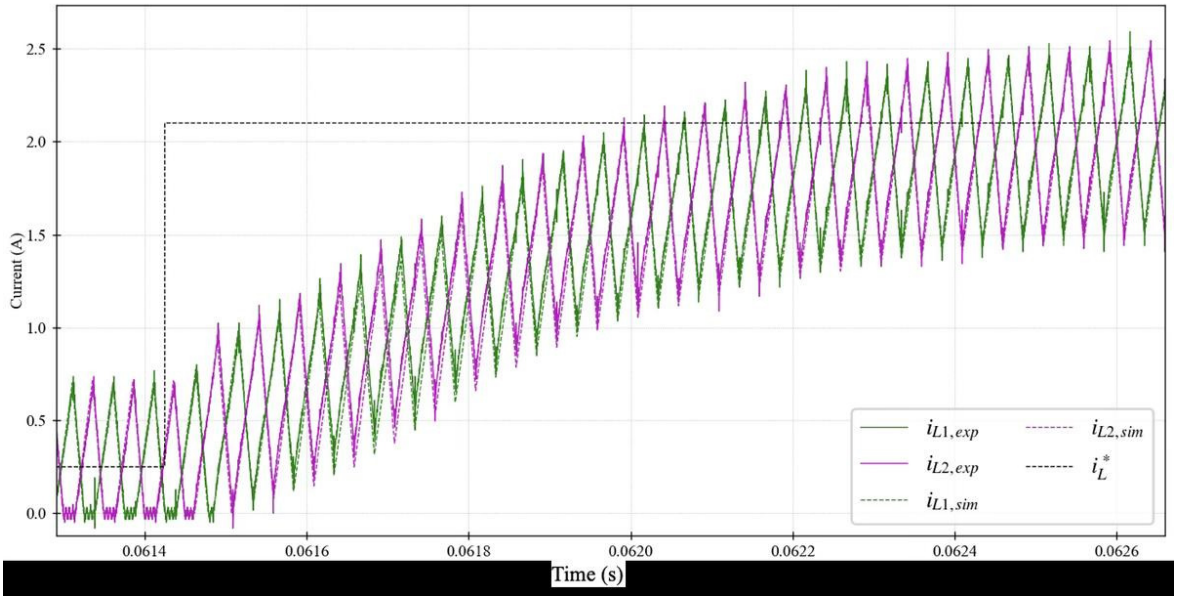

Figure 5. Simulation and experimental results of the proposed current-controller.

Power-sharing during maximum state-of-charge conditions of the battery system.

Two approaches to address the operational limitations of the upper end of the battery state-of-charge (SoC) range in standalone mode were developed. The first method allows the battery to be charged at a specific C rate, which is one of the possible charging strategies for the upper end of the SoC. Additionally, the method allows disabling battery charging during steady state, using it as a backup during transients.

The second method targets the hard limit of the SoC, when no more energy must be transferred to the battery, to preserve the battery health. In this case, the battery converter is disabled, and the PV system maintains the power balance. The transitions from normal operation to the maximum SoC condition and vice versa are validated, as are the operations during load changes. Experimental results of the proposed power-sharing strategy are shown in Figure 6. At 60 ms, the battery reaches the maximum SoC, as observed in Figure 6(c), and as a consequence, the proposed power sharing technique is enabled.

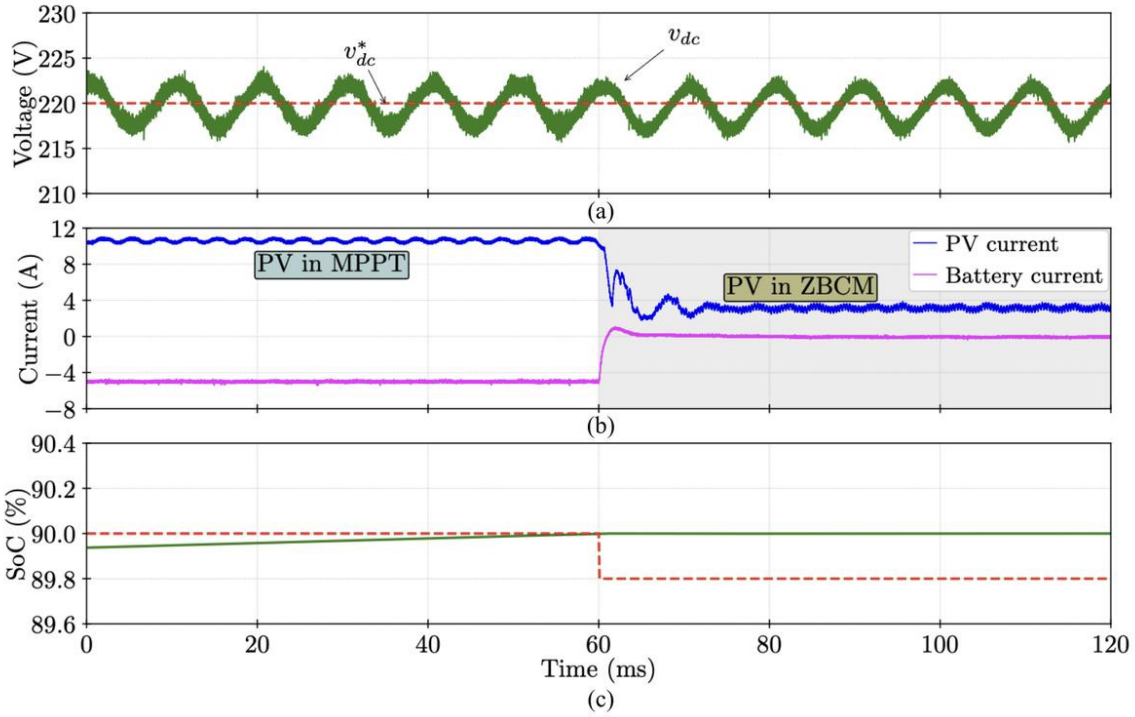

Figure 6. Power-sharing under maximum SoC. (a) dc-link voltage. (b) dc-dc sources currents. (c) SoC.

In this condition, the battery current reaches an average value of 0 A after the transition. In contrast, the PV system maintains the power balance in the system by changing the operating point, which is observed in Figure 6(b). Despite the transition, the dc-link voltage remains unaffected, as presented in Figure 6(a). With the proposed power-sharing strategy, the system operation is maintained, and overcharging of the battery can be avoided without affecting the operation of the ac side, since the dc-link voltage remains stable.

Constant power at the PCC

Instead of operating each unit individually, an alternative solution to provide constant power at the PCC of the studied system with PV, battery and manageable loads was developed. In the proposed method, the system operates in a coordinated manner to provide or absorb a specified amount of active power over a specified time as a single unit. As a result, from the perspective of the coordination unit in centralized architectures, the system can be commanded as a single unit rather than controlling each element separately. This could potentially benefit the scheduling algorithms, since the number of variables of the problem is reduced.

To achieve the requested power set point, the proposed solution comprises three parts. First, a power controller that allows the system to follow the requested grid power reference. The second element is a higher-level algorithm that determines the feasibility of the request, and determines the power reference for the PV system and the status of the manageable loads. Lastly, a flexible power point tracking (FPPT) algorithm with adaptive step, which allows the PV system to deliver the power reference determined by the higher-level algorithm, was developed.

Simulation results of the proposed active power controller are shown in Figure 7. Initially, the PV system operates in maximum power point tracking (MPPT) mode with an output power of 2.5 kW. Meanwhile, the load power is set at 2 kW, and the system operates in self-sufficiency mode, resulting in a grid power of 0 kW, since the battery compensates for the power difference. Then, 0.1 s the grid power reference is set at -3 kW for a time of five seconds. Consequently, the reference power of the PV system is set at 1.2 kW. The battery initially provides the power to achieve the requested grid power reference, while the PV system slowly changes the operating point, as shown in Figure 7(a). After 0.5 s, the output battery and PV power are set at -1.1 and 1.2 kW, respectively. Additionally, both loads are enabled since the request is feasible. After providing the requested support, the battery reaches the maximum SoC and the system returns to self-sufficiency mode, and the PV converter returns to MPPT operation.

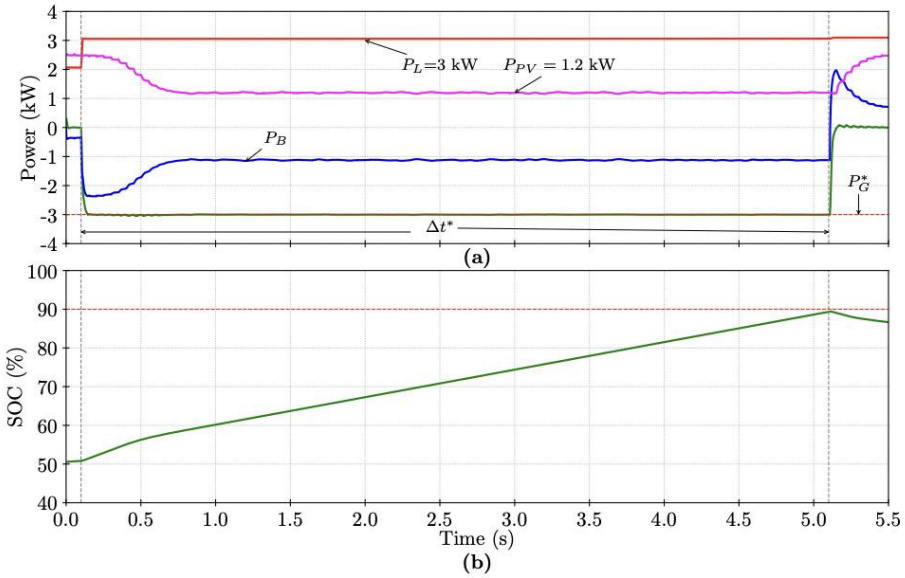

Figure 7. Proposed active power controller for a grid reference power of -3 kW.

Comparison of Energy Management Systems.

The development of an Energy Management System (EMS) designed as a hierarchical control layer that bridges high-level optimization with the lower-level controllers, was conducted. Two different objectives were compared. Energy Cost Minimization: Reducing the electricity bill. Self-Consumption Maximization: Optimizing the utilization of local PV generation to minimize energy exchanged with the grid.

Initially, the formulated problems were solved with a Genetic Algorithm (GA). This metaheuristic approach leverages next-day forecasting and continuous search space to determine optimal dispatch schedules, ensuring that the system maintains a desired State of Charge (SoC) at the end of the day. Additionally, the GA-based optimizer was compared to a deterministic graph-based approach formulated through the discretization of the battery SoC. The comparison demonstrated that the graph-based method offers a significant advantage in execution speed at the cost of memory requirements, providing a deterministic solution suited for real-time implementation. Simulation results for one alternative of the proposed EMS are shown in Figure 8, for an analysis of two consecutive days with different irradiance conditions, aiming to minimize energy exchange with the grid.

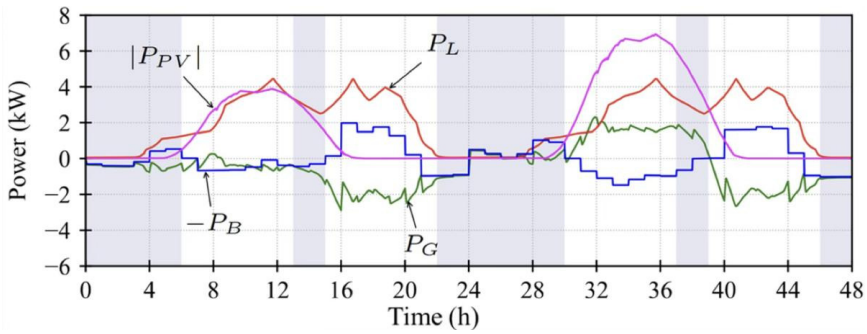

Figure 8. Simulation of energy management for energy exchange minimization.

The presented contributions have been extensively disseminated through peer-reviewed journals, and presented at international conferences, reflecting the impact of the project on the improvement of the operation regarding renewable energy systems. A comprehensive list of the resulting publications and dissemination activities is provided in the following section

3.2.3. Contribution to the WP objectives

The development and implementation of the EMS contributes to the first objective as part of the new ways of managing electric generation using renewable energy. In this study, the selected source is a PV module. Additionally, the development of the prototype is also a contributing factor to this objective since this prototype enables the integration of new electricity generation technologies into the existing electricity generation paradigm.

The design and implementation of the appropriate mechanisms to identify faults and the execution of control algorithms contribute to the second objective, which is to design the best and safest ways to integrate renewable generation into the existing grid.

Contribution to the third objective corresponds to the development of control algorithms, as this is the part of the prototype in which the coordination of different and complementary sources is carried out.

3.2.4. Scientific achievements

Experimental prototypes

#	Name	Description	Status	Photo
1	PV and Battery based residential system.	Power converter to integrate PV arrays and batteries to	Tested	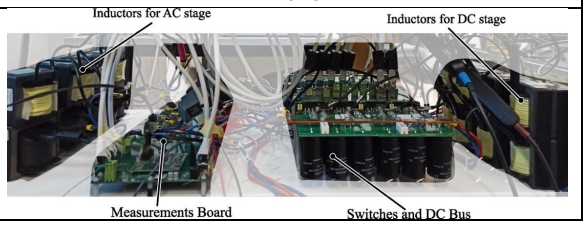

Publication

#	Title	Type	Status	DOI
1	Comparison of Energy Storage Management Techniques for a Grid-Connected PV- and Battery-Supplied Residential System	Journal	Published	10.3390/electronics13010087.
2	A Control Strategy for a Standalone PV-Battery System Operating at SoC Boundaries With DC-Link Ripple Management	Journal	Published	10.1109/ACCESS.2025.3625405.
3	A Current Control Method for an Interleaved Boost Converter Under CCM/DCM Operation in a PV System	Conference	Published	10.1109/CPE-POWERENG60842.2024.10604371
4	Control Strategy of Hybrid Energy Storage System for High-Dynamic Load Changes	Conference	Published	10.1109/CPE-POWERENG58103.2023.10227479
5	Converter Averaging Approach for Modeling a Residential Supply Subsystem	Conference	Published	10.1109/CPE-POWERENG58103.2023.10227486
6	Grid Active Power Control with Optimal Battery Usage and Demand Side Management	Conference	Published	10.1109/CPE-POWERENG63314.2025.11027282
7	Soft-Start Method for Boost Converter Under Rapid Irradiance Changes	Conference	Published	10.1109/IECON55916.2024.10905290
8	An Intentional Islanded Mode of Operation for a Four-Leg Converter Under Rapid and Asymmetrical Load Changes	Conference	Published	10.1109/IECON55916.2024.10905463

3.3. Task 2.3 – IRP3 "Virtual Power Plant for operation, both isolated and connected"

3.3.1. Introduction

The ESRs associated with the deliverable: ESR03 (Anas Abdullah Alvi) coordinated by the University of Extremadura (UEX) with IRP03 "Virtual Power Plant for operation, both isolated and connected" with the following goals: A graphical interface-based Application of VPP Digital Twin using MATLAB App Designer that can perform the Energy Management System (EMS) optimization (economical and/or technical) of the distribution grid by using Genetic Algorithm, producing operation set points for microgrid resources as, for example, start on/off times, MPPT or RPPT for PV facilities, charging and discharging of ESS or EV.
The scientific outcomes have been obtained during 30 months in the facilities of the PE and ES Research Group of the University of Extremadura, Spain, 2 months in the Power Electronics Group of Tallinn University of Technology, Estonia and 4 months in the Power Electronics Group of Warsaw University of Technology, Poland with visits to industry (LOPI) to develop the business model. The main research work was started by performing a complete literature review of Virtual Power Plants (VPP). This was followed up by writing a review paper on some of the functions and roles of VPPs. After completing the literature review, a case study was performed in which simulation work was done by using MATLAB Simulink. The main idea of this case study was to get familiarized with the design and performance of a grid connected PV inverter consisting of single-phase unbalanced loads and observing its effects in different points of the microgrid. Next research work was followed up with a genetic algorithm developed and tested to control the energy storage system and the charging and discharging of electric vehicles consisting of technical and financial goals. The next and final work focused on improving the algorithms and developing of the VPP Application prototype by using MATLAB App designer software including a Graphical User Interface (GUI) of the system. Moreover, 2 collaborative outcomes were achieved together with ESR 01 among which the first is a published conference paper that focusses on the guidelines of the use of Genetic Algorithm in Energy Management System and the second is a journal published in 'Energies' based on the random behaviour of GA and its improvement together with a validation of a microgrid by using PLECS simulation software. A collaborative outcome is also achieved by means of a conference contribution together with ESR 14 based on techno-economic feasibility of VPPs.

3.3.2. Scientific outcomes

The virtual power plant (VPP) is the integration of distributed energy resources (DER) under a coordinated management system. A VPP is an interconnected network of decentralized, small-scale power resources, such as solar panels, wind turbines, power converters, energy storage systems and manageable loads that work together under the control of an aggregated control system. Like a conventional centralized power plant, the VPP may be regulated to adapt to changes in energy demand and supply and can offer grid services like balancing and stability. The purpose of this integration of dispersed energy resources into a unified utility grid is to improve the energy system's dependability, flexibility, and efficiency.

Large, centralized generation units were intended to be managed by the power system so that real-time monitoring and control of their safe operation and dependability was possible. Renewable energy sources (RES), such as solar, wind, and hydro power, have been growing in popularity due to their environmental benefits and decreasing costs. However, their integration into existing power systems has presented new challenges for control and operation. The overwhelming amount of information including weather forecasts, power demand, and supply, that operators must process in real-time and the dependability of the power electronics-based systems working in parallel, as hundreds of power converters would be simultaneously exchanging energy with the grid, is the main obstacle to increasing the expansion of RES. In practice, it has already been observed that generation systems powered by power converters are having an impact on the stability and dependability of power systems due to the dynamics of the converter not matching well with the dynamics of the grid or due to the introduction of voltage and current harmonics into the power system. Even though distributed RES-based units are currently only considered because of their modest involvement, this will change soon due to the rapid increase in RES integration and the diminishing situation of fossil fuel power facilities. To balance generation and demand while also contributing to the stability of power systems, utility-scale renewable power facilities must be designed and operated in a certain method.

The main objectives of the developed prototype of a VPP software application are given below:

- To create and evaluate VPP that groups and optimizes resources from several microgrids (MG). MGs could include household and industrial loads, photovoltaic generation (PVG), energy storage systems (ESS), and bidirectional electric vehicles chargers (V2G).

- The main objective is to develop an **Energy Management System (EMS) of VPP** to do an economical and/or technical optimization of the distribution grid by using **Genetic Algorithm**, producing **new operation set points** for microgrid resources as, for example, start on/off times, MPPT or RPPT for PV facilities, charging and discharging of ESS or EV.
- This study proposes a **novel VPP** for a residential microgrid (MG) equipped with an ESS and EV, aimed at reducing electricity costs.
- The proposed VPP employs a **two-stage optimization framework** that integrates **economic objectives** while satisfying the **operational constraints**.
- Specifically, the optimization problem incorporates the optimal scheduling of EV charging and discharging during off-peak (valley) hours to **minimize electricity bills**, as well as the strategic dispatch of ESS power to the grid either by supplying energy during peak hours or drawing energy during valley hours.
- In the first stage, a **GA** is used to explore the solution space, recognizing the stochastic nature of GA results; therefore, executing the algorithm several times to ensure the robustness of the solution.
- In the second stage, a GBM, specifically the **F_{mincon} solver** from MATLAB, is applied to refine the solution due to their computational efficiency. Any remaining unmet constraints are subsequently resolved through analogous correction in the last hour of operation.
- To **validate** the proposed approach, a real-world case study is conducted, demonstrating the effectiveness of the method in achieving economic objectives while satisfying all the defined operational constraints.
- Then, the functionality of the proposed VPP is evaluated using a detailed system model that incorporates **PECs** along with their associated low-level controllers.
- The appropriate **optimization functions and constraints** are identified that includes the provision of ancillary services.
- A **graphical interface**-based Application using **MATLAB App Designer** for the whole algorithm, which collects the data of each microgrid (generation, demand, data of batteries and EVs…) and provides the optimal setpoints for EV and batteries power.
- Finally, a detailed business model is proposed for the implementation of the developed application of the VPP.

3.3.2.1 Control algorithms and firmware of the prototype

The prototype consists of a VPP that manages two MGs that integrates Household Loads, PVG, ESS and V2G, to define the power profiles with a minute's resolution and to determine the set-points for each resource in each microgrid. The number of PMGs and VPPs can be modified according to the needs of the user. The developed VPP can be demonstrated below by using a simple block diagram in fig 1.

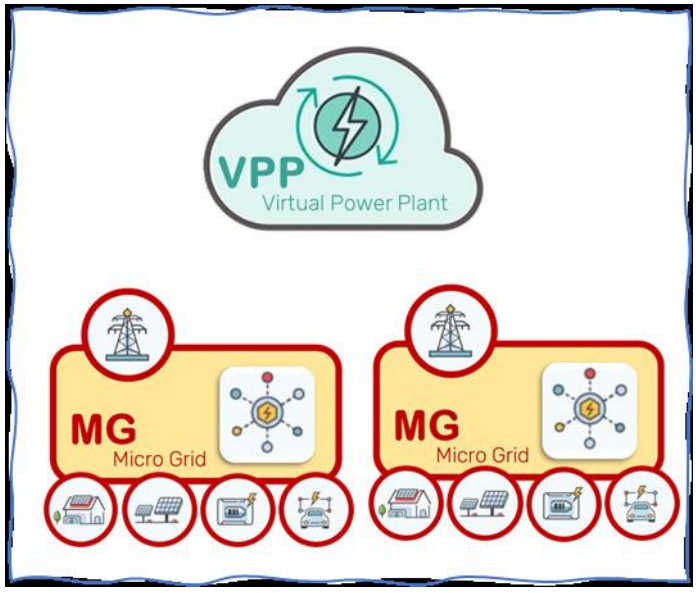

Fig 1. Developed VPP under study.

The VPP under study encompasses:

Microgrid 1:

- Households: 8 houses with different demand profiles
  - 4 houses were modelled with a medium level of annual electricity use.
  - 4 houses responded to a high-demand profile.
- A PV power plant rated at a 15-kW peak.
- An ESS with a capacity of 24 kWh, maximum charge/discharge power of ±6 kW and a SoC range of 20–100%.
- Four EVs, each with a battery capacity of 50 kWh.

Microgrid 2:

- Households: 1 house.
- A PV power plant rated at a 15-kW peak.
- An ESS with a capacity of 24 kWh, maximum charge/discharge power of ±6 kW and a SoC range of 20–100%.

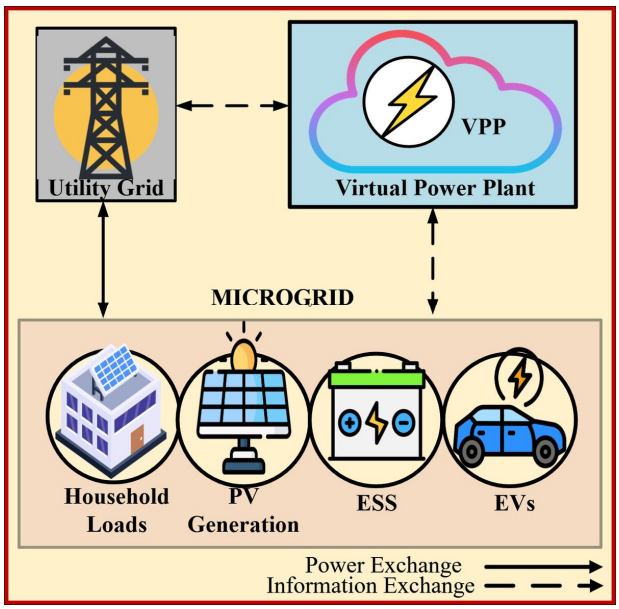

Fig 2. Elements of the MG under study.

The main elements of the MG as discussed in MG1 and MG2 are shown in fig 2. The main objective of the designed algorithm is to optimize the energy interchange between the MG and the VPP so that the electricity bill is reduced by using GA. Some parameters of the charging/discharging of the EVs are also defined in such a way that they are charged during the valley/ off-peak hours between 12am to 8am to reduce electricity bill. Also, the EMS should supply electricity to the grid when the price of electricity is high and charge itself when the price is lower.

3.3.2.2 Control algorithms and firmware of the prototype

The main control algorithm of the prototype is divided into 2 parts. In the first part, a genetic algorithm with appropriate constraints is designed and tested to manage the energy storage system and the charge/discharge of electric vehicles, with several economic and technical objectives. The second part is focused on developing the VPP application by using MATLAB App designer to create a GUI based digital twin of the VPP. Both control algorithms are discussed in detail in this section.

3.3.2.3 Optimization Algorithm:

The optimization algorithm is the first step towards designing the VPP Digital Twin Application. The flowchart of the steps followed in optimizing the electricity costs between the VPP and the MG are shown in fig 3.

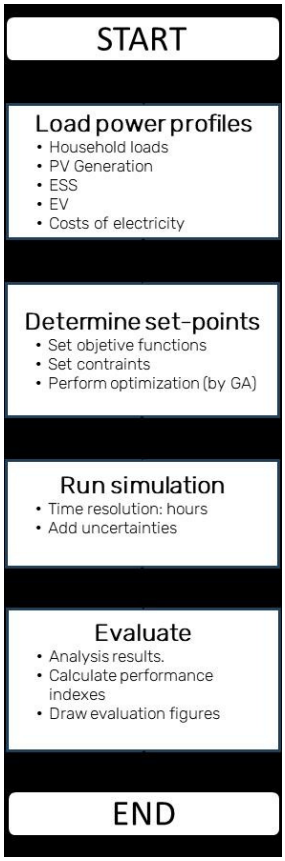

Fig 3. Flowchart of steps followed in optimization of electricity costs.

To determine the new set points of operation for the ESS and the EVs in order to reduce electricity bill, the proper objective function and constraints must be defined accordingly [3].
The VPP power balance is defined in (1). Starting from (1), the objective functions are shown in (2) and (3).

$$P_{grid}(h) = P_{PV}(h) - P_{LD}(h) - P_{ESS}(h) - P_{EV}(h) \quad (1)$$

$$f_1 = \sum_{h=1}^{24} P_{grid}^2(h) \quad (2)$$

$$f_2 = \sum_{h=1}^{24} \left[\left(I_{pur}(h) \cdot p_{pur}(h) - I_{sel}(h) \cdot p_{sel}(h) \right) \cdot \left| P_{grid}(h) \right| \right] \quad (3)$$

Objective function f1 in (2) aims to minimize the power interchanged with the grid. It is useful to maximize SC and SS without considering prices, for example, in TVPP devoted to supporting the distribution grid. CVPP requires economic incentives for final users to be motivated to participate in the VPP; in these kinds of VPP, objective function f2 in (3) is more appropriate, which aims to minimize the VPP electricity bill. While designing the final VPP prototype, only the objective function of minimizing the electricity bill is considered to be included in the GUI.
Constraints for ESS are shown in (4)-(6).

$$-P_{ESSmax} \leq P_{ESS}(h) \leq P_{ESSmax} \quad (4)$$

$$SoC_{lo} \leq SoC(h) \leq SoC_{up} \quad (5)$$

$$|SoC_{in} - SoC(24)| \leq 10\%, \quad (6)$$

where:

$$SoC(h) = SoC_{in} + \sum_{i=1}^{h} \left(I_{ESSch}(i) \cdot P_{ESS}(i) \cdot \eta_{ch} + I_{ESSdi}(i) \cdot \frac{P_{ESS}(i)}{\eta_{di}} \right). \quad (7)$$

Constraint in (4) delimits the allowed range of power of the ESS. The maximum power of the associated power converter P_{ESSmax} is considered, and both positive (charge) and negative (discharge) power values are allowed. On the other hand, (5) delimits the allowed *SoC* range according to manufacturer recommendations, and (6) guarantees that the difference in *SoC* between the beginning and the end of the day is lower than 10%. Other works ¡Error! No se

encuentra el origen de la referencia. propose equal values for these *SoC* values, to complete a daily charge/discharge cycle. However, this constraint reduces the flexibility of the model. With a maximum difference of 10%, it can be avoided that the ESS is completely charged or discharged at the beginning of the next day, with a certain flexibility. The ESS *SoC* is calculated as in (7), considering both charge and discharge efficiency rates.
On the other hand, constraints for EV power are shown in (8)-(10).

$$-P_{EVmax} \cdot n_{EV}(h_{EV}) \leq P_{EV}(h_{EV}) \leq P_{EVmax} \cdot n_{EV}(h_{EV}),\ h_{EV} \in nh_{EV} \quad (8)$$

$$P_{EV}(h) = 0, h \notin nh_{EV} \quad (9)$$

$$\sum_{h_{EV}} P_{EV}(h_{EV}) = E_{EVtotal}. \quad (10)$$

There is a time restriction for EVs. They can only be charged/discharged during the time slot they are connected to the grid and available for charging/discharging. During these hours, the maximum power is limited to that of individual chargers multiplied by the number of connected vehicles, as in (8). For the remaining hours, the power for EV is zero (9). Constraint in (10) guarantees that, at the end of the time slot the EVs are connected to the grid, the whole energy amount necessary to fully charge all the EVs has been charged, i.e., SoC for every EV must be 100%.
The objective function and its constraints related to the 2nd stage optimization of gradient based method is based on equations (11-15).

$$min\ f_2(x) = \sum_{h=1}^{24}[f_1(h)] \quad (11)$$

The function to be minimized is the objective function f_2, which usually represents a cost objective and receives input from the GA's first stage of optimization. For this optimization issue, the limitations related to the SoC of the EVs and ESS are regarded as being the same as earlier. In this case, x can be described as:

$$x_{k+1} = x_k - \alpha \nabla F(x_k) \quad (12)$$

Here, x_k is the decision variable at iteration k, representing power dispatch decisions, α is the step size (learning rate), and $\nabla F(x_k)$ is the gradient of the objective function, given by:

$$\nabla F(x) = \frac{\partial F(x)}{\partial P_{grid}(h)} \quad (13)$$

For each time step h,

$$\frac{\partial F}{\partial P_{grid}(h)} = I_{pur}(h) \cdot p_{pur}(h) - I_{sel}(h) \cdot p_{sel}(h) \quad (14)$$

Ultimately, following the second optimization stage, it is evident that the EV's SoC constraint is not entirely met. To analogously satisfy the necessary constraint of EVs, the following equation (14) is utilized.

$$E_{EVtotal} = E_{EVtotal} + \max(30000 - E_{EVtotal}) \quad (15)$$

Here, the remaining power is provided from the grid to fully charge the EVs during the final hour (7 to 8 hours) if their total SoC does not reach 30 kWh at the end of 8 hours.

3.3.2.4 VPP GUI Algorithm

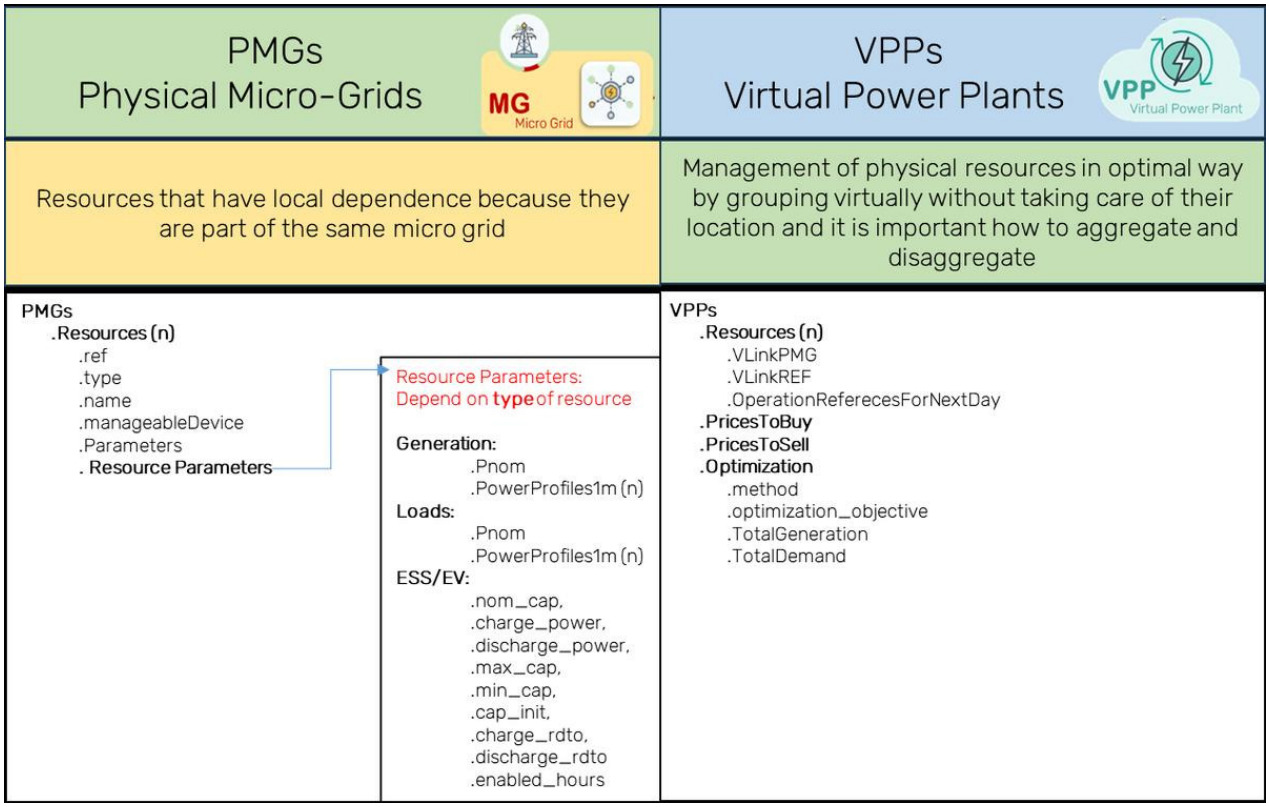

The system is described in two level:

- Physically: The electric system is divided in microgrid (physical microgrids: PMG).
  PMG integrates resources.
  Resources are defined following the structure described in Table I that is mainly programmed in file **ResourceParameters.mlx**.

Table I. Resources description: ResourceParameters

Variable	Description
.ref	Is the reference of the resource for a better understanding or following of the simulation or for selecting the resource in the library of resources
.type	Is the type of resources. There are three types in version V0: • generation • load • ess
.name	The name could be given by user to identify uniquely the resource
. manageableDevice	True or false depending if the resource is manageable or not.
.Parameters	There are specific parameters that depend on the resource type of reference
.PowerProfiles1m	Power profiles with a minute resolution. They could one more than one profile and they could cover different time intervals (days, week)

Table II. Parameters for resource of type "generation"

Variable	Description
.Pmax	Peak power of the generation curve

Table III. Parameters for resource of type "loads"

Variable	Description
.House1	Load the demand profile of the first house
.House2	Load the demand profile of the second house

Table IV. Parameters for resource of type "ESS"

Variable	Description
. PchargeMax .PdischargeMax	To define the maximum charging and discharging power of the ESS
. Capacitiy	To define the power capacity of the ESS
SOCmin	Defines the minimum state of charge of the ESS at the end of the day

Table V. Power profile description: PowerProfiles

Variable	Description
.PVGen	It loads the power profiles of the generators. In this case, there are two generation plants as follows: PVG1.mat PVG2.mat
. House	It loads the power profiles of the houses. In this case, there are two houses as follows: House_ERC_PowerProfiles_1week_2013may.mat House_SEB_PowerProfiles_2week_2013may.mat

- Virtually: The VPP simulator consists of DERs, ESS, household loads and EVs. It creates new operation set points for the ESS and EVs.

Resources: Parameters to perform the optimization are defined following the structure described in the following tables that is mainly programmed in file VPP_case0_definition.mlx

Table I. Parameters description: VPP_case0_definition.mlx

Variable	Description
.EnergyByHour	It loads and initializes the power profiles for: • generation • load • ess

Table II. Parameters description of ESS: VPP_case0_definition.mlx

Variable	Description
.nom_cap	Nominal capacity of batteries (Wh)
.charge_power	Max charging power of batteries (W)
.discharge_power	Max discharging power of batteries (W)
.max_cap	Max SoC of batteries, SoC=100% (Wh)
.min_cap	Min SoC of batteries, SoC = 20% (Wh)
.cap_init	Initial charge of batteries, SoC=50% (Wh)
.charge_rdto	charging efficiency rate
.discharge_rdto	discharging efficiency rate

Table III. Parameters description of EVs: VPP_case0_definition.mlx

Variable	Description
.nom_cap	Nominal capacity of 4 EVs (W)
.charge_power_EV	Max charging power of 4 full power chargers (W)
.discharge_power	Max discharging power of 4 EVs (W)
.max_cap	Max capacity of EV batteries, SoC=100% (Wh)
.min_cap	Min charging of EV batteries, SoC = 50% (Wh)
.charge_rdto	charging efficiency rate
.discharge_rdto	discharging efficiency rate

Table IV. Parameters description for visualization: VPP_case0_definition.mlx

Variable	Description
VLinkPMG	To display the resources of MGs
VLinkREF	To display the results of the resources

Table V. Parameters description of prices: VPP_case0_definition.mlx

Variable	Description
.PricesBuyHour	To load the buying prices by the VPP
.PricesSellHour	To load the selling prices by the VPP

3.3.2.5 Simulation verification of the prototype

Optimization Results: In the initial optimization problem, 4 different cases were considered such as minimization of power interchange with the grid, minimization of electricity bill, minimization of electricity bill subjected to grid constraints and multi-objective optimization. However, in the final prototype, only the case of minimization of electricity bill is considered due to the simplicity as well as highest reduction of electricity bill among all the cases as shown below.

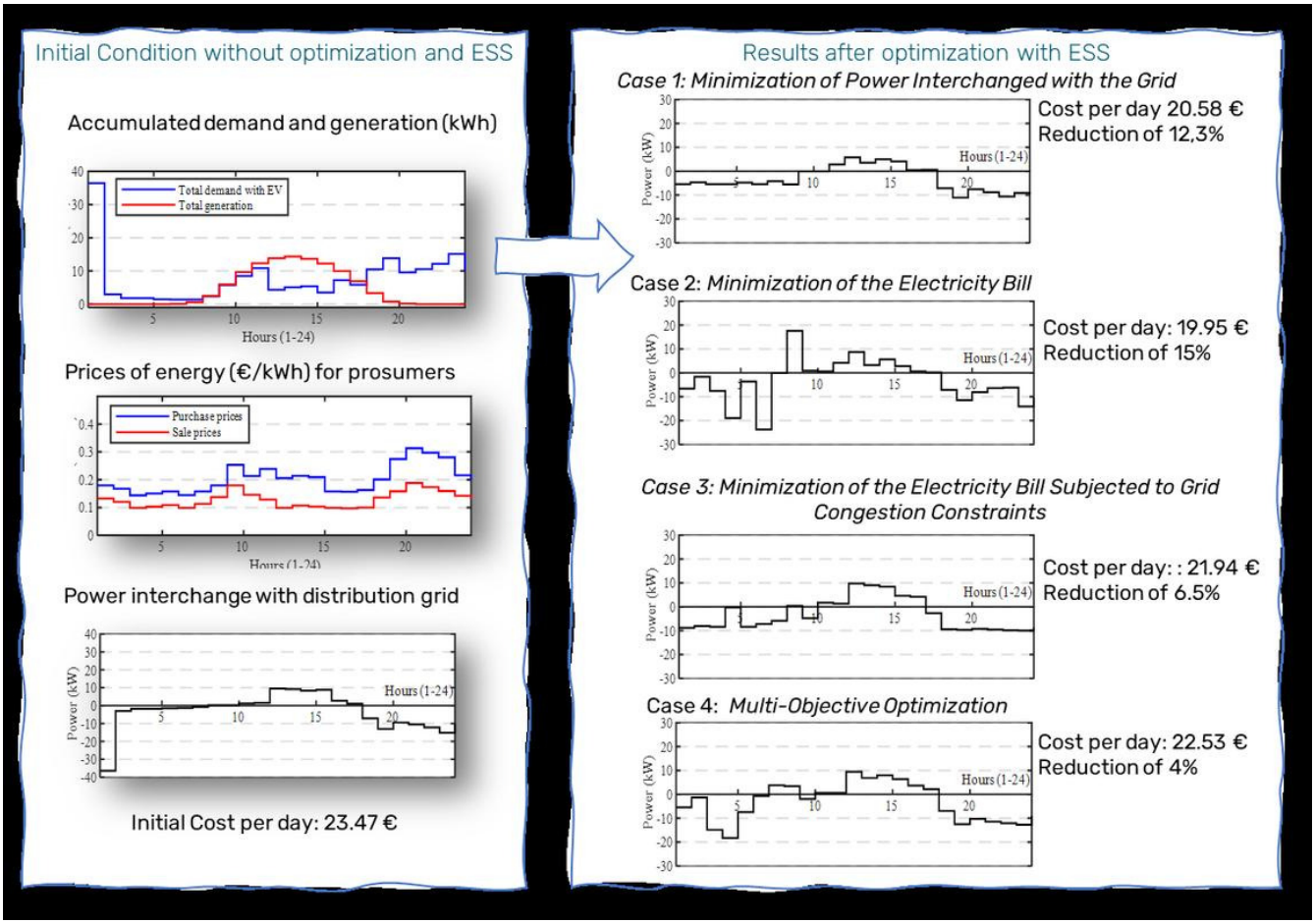

Figs. 4 to 6 show the results obtained by the GA when objective function f_2 in (3) and constraints (4)-(6) and (8)-(10) are used.

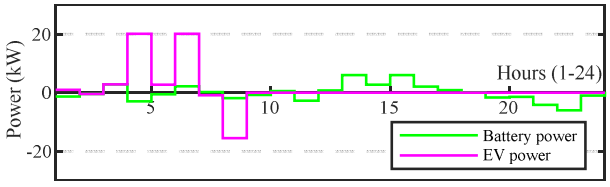

Fig 4. Power scheduled for ESS and EVs, case 2.

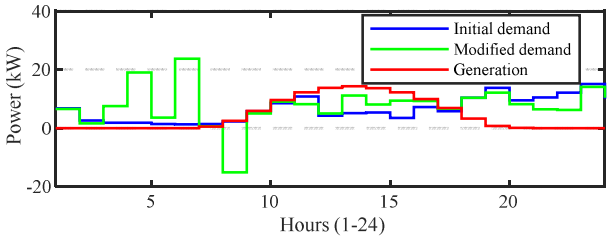

Fig 5. Accumulated demand and generation after scheduling, case 2.

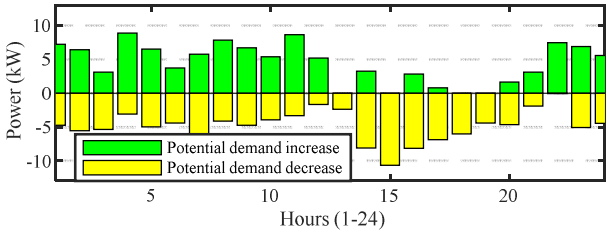

Fig 6. Potential increase/decrease of ESS power for AS, case 2.

Observation of Fig. 4 leads to verification that the EV charging/discharging at each night hour is sharper to adapt to different prices at each hour without peak-shaving purposes. In this case, the operation of ESS is devoted to avoiding buying high amounts of energy at the highest-price hours. Therefore, the interchange of power with the grid has higher peaks. The highest peaks for bought energy coincide with low price hours (middle night and last hour). It is interesting to highlight that during the last hour of the day, the ESS has not provided most of the energy demanded by loads by storing more energy produced by the PV during the midday. That is because the price for the purchased energy at the end of the day is similar to those of the central hours of the day, whereas extra PV production can be sold at these central hours. In this case, SC is 58.16%, SS is 39.19% and the final bill is 19.95 €/day (a reduction of 15% starting from the base case). This bill is the lowest among the studied cases detrimental to SC and SS rates.

3.3.2.6 2 Stage Optimization and Constraint Adjustment

In the second stage of optimization, a Gradient-Based Method (GBM) namely the F_{mincon} solver from MATLAB is used to refine the results after the 1st stage and further improve the cost minimization as well as fulfilment of the constraints. It could be observed that one of the constraints i.e. the SoC of the EVs was not fulfilled in the previous method. Hence, it was manually adjusted in this method. The method is shown in the figure below in figure 7.

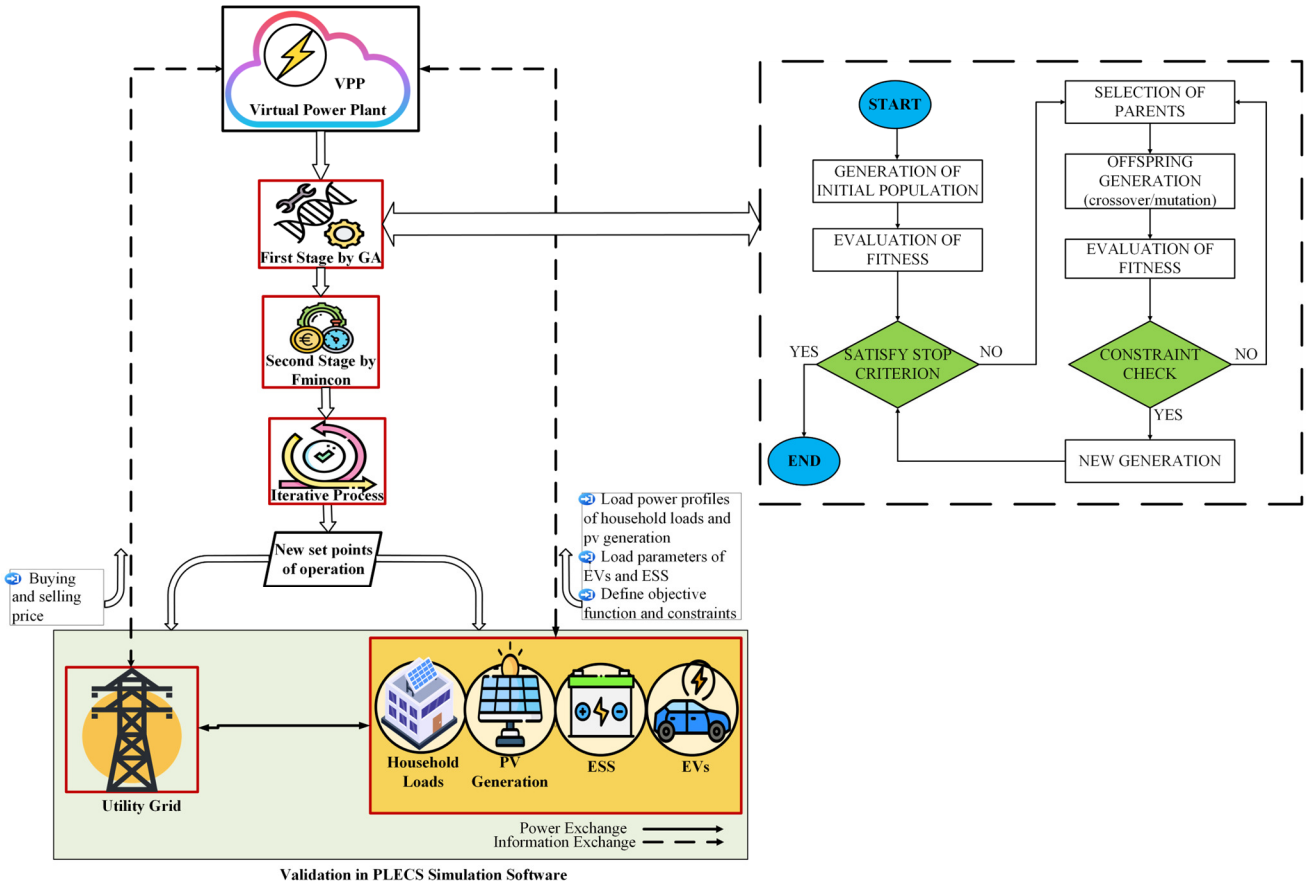

Figure 7. Strategy of two stage optimization procedure.

After performing the simulation, the following result is obtained as shown in figure 8.

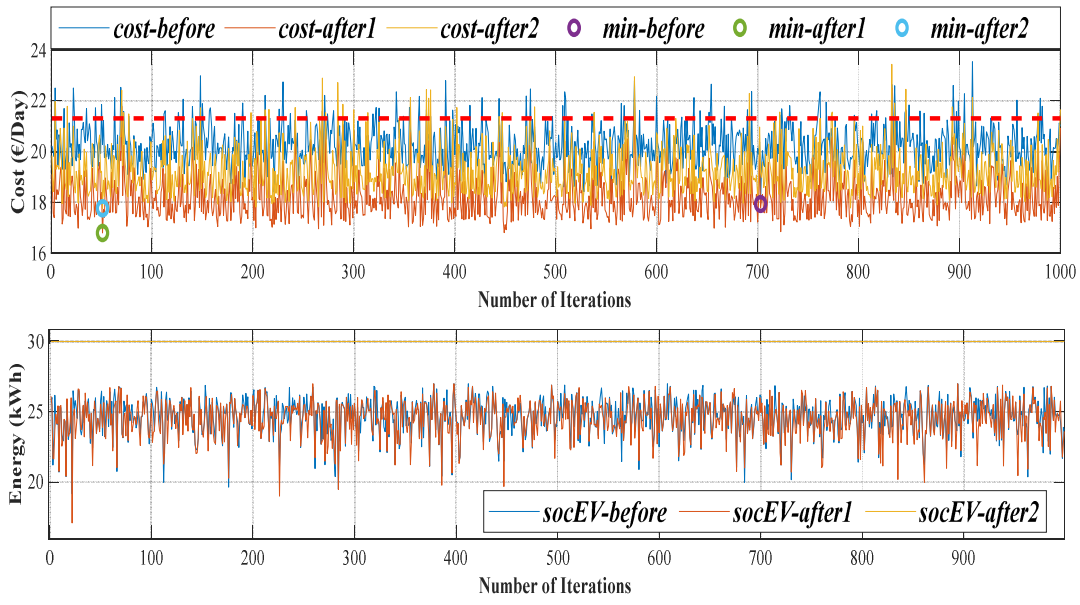

Figure 8. Number of iterations versus change in cost.

After performing 1000 iterations, it can be observed that, after the 1st stage of only using GA, the minimum cost is 17.9375 euros after try number 703. After the 2nd stage of using GA and F_{mincon}, the minimum cost is 16.7925 euros after try number 51. After adjusting the EV SoC constraint, the minimum cost is 17.7674 at try number 51. This cost is

a reduction of 24.3% from the base case (an improvement of 9.3% when only using GA as well as fulfilling the SoC constraint in this case).

3.3.2.7 Validation using PLECS Simulation Model

This section consists of the validation of the obtained set points of operation after performing the optimization by using a detailed system model that incorporates PECs along with their associated low-level controllers. The simplified diagram of the developed model is shown in Figure 8(a). Figure 8(b) depicts a residential grid-connected system with PV generation and a lithium-ion battery serving as the ES device for this study. A bidirectional converter connects the battery to the DC bus, and a boost converter interfaces the PV module with the system. Operationally, both DC-DC converters are interleaved. Because of its capacity to lessen the current load on semiconductor components, this topology was selected. Additionally, interleaving enables a fourfold reduction in filter size while preserving the same input current ripple compared to traditional converter arrangements.

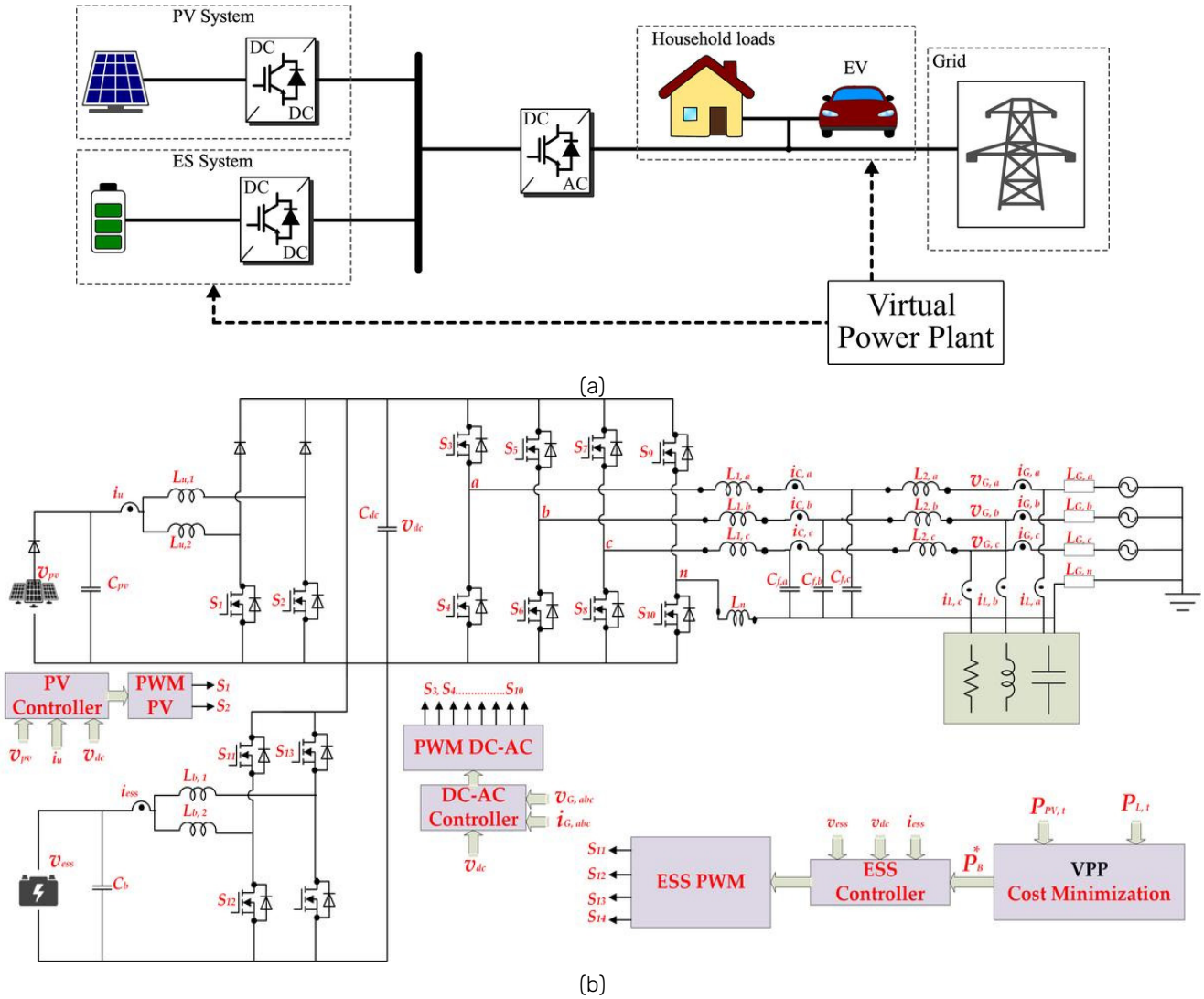

Figure 8. (a) Simplified diagram of the residential system under study,
(b) Schematic diagram of the residential system under study.

3.3.2.8 Results from PLECS simulation model

The proposed control strategies must be computed in advance to define the battery's scheduled power profile. This involves determining an hourly reference power P*B,t, which is updated on an hourly basis and transmitted to the ESS controller. The battery's SoC is estimated by using the Coulomb counting method. The acquisition of power profile data is enabled by the widespread deployment of smart meters. This study adopts an hourly resolution for

both load and generation pro-files. Notably, the proposed methodology is adaptable and can be extended to finer time intervals by modifying the relevant constraints and providing appropriately resolved in-put data. Here, the constraints are selected according to the previous case and the inputs are taken from the final optimal output is fed to the PLECS simulation model. For simplicity, the EV is considered as a current source in the model during simulation that supplies or demands power according to the references from the optimal results. It can be observed from Figure 11 that, after taking the references of operation of the ESS and EV from the optimal solution, the model behaves in an ideal way and the reference set-points are followed. The total cost of energy obtained in this way deviated by only 3.85%.

3.3.3. Contribution to the WP objectives

According to the grant agreement, deliverable D2.3 is a prototype of virtual power plant that can operate both isolated and grid connected mode. The prototype of the VPP control is composed of 2 sections. The first component consists of optimizing the energy interchange between the VPP and the MG in order to lower the power cost, which is one of the functions of the Energy Management System (EMS). The second step is to create a GUI-based digital twin of the VPP in which the number of MGs and VPPs, as well as the elements, can be changed to meet the user's requirements. This digital twin can optimize the outcomes using the first part's algorithm and display them in a user-friendly format that is easy to understand.

3.3.4. Scientific achievements

Experimental/Software prototypes

#	Name	Description	Status (designed, assembled, tested)	Photo
1	Digital twin of the VPP	A graphical interface-based Application using MATLAB App Designer for the whole algorithm, which collects the data of each microgrid (generation, demand, data of batteries and EVs…) and provides the optimal setpoints for EV and batteries power.	Completed	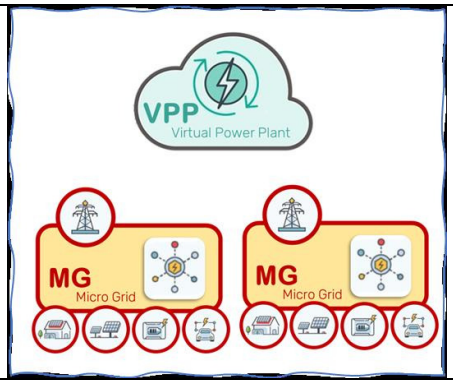

Publication

#	Title, incl. citation information	Type (Conference, journal, book chapter)	Status (Submitted, accepted, published)	DOI
1	Alvi, A.A., Romero-Cadaval, E., González-Romera, E., Hassan, J., Vinnikov, D. (2023). An Overview of the Functions of Smart Grids Associated with Virtual Power Plants Including Cybersecurity Measures. Technological Innovation for Connected Cyber Physical Spaces. IFIP Advances in Information and Communication Technology. Springer 2023, ISBN: 978-3-031-36006-0	Book Chapter	Published	https://doi.org/10.1007/978-3-031-36007-7_7

2	A. A. Alvi, E. Romero-Cadaval, E. González-Romera, D. Vinnikov and J. Hassan, "Performance Evaluation of a Three-Phase PV Power Plant under Unbalanced Conditions with Islanding Detection Reliability Test," 2023 IEEE 17th International Conference on Compatibility, Power Electronics and Power Engineering (CPE-POWERENG), Tallinn, Estonia, June 2023, pp. 1-6,	Conference	Published	doi: 10.1109/CPE-POWERENG58103.2023.10227391.
3	González-Romera, E.; Romero-Cadaval, E.; Roncero-Clemente, C.; Milanés-Montero, M.-I.; Barrero-González, F.; Alvi, A.A. A Genetic Algorithm for Residential Virtual Power Plants with Electric Vehicle Management Providing Ancillary Services. Electronics 2023, 12, 3717.	Journal	Published	https://doi.org/10.3390/electronics12173717
4	A. A. Alvi, E. González-Romera, E. Romero-Cadaval, D. Vinnikov, M. I. Milanés-Montero and F. Barrero-González, "An Economical Optimization for the Participation of a Residential Microgrid in Flexibility Markets Providing Ancillary Services," 2024 IEEE 18th International Conference on Compatibility, Power Electronics and Power Engineering (CPE-POWERENG), Gdynia, Poland, 2024, pp. 1-6, doi: 10.1109/CPE-POWERENG60842.2024.10604394.	Conference	Published	doi: 10.1109/CPE-POWERENG60842.2024.10604394.
5	J. Hassan, V. Minambres-Marcos, F. Barrero-Gonzalez, A. A. Alvi, M. Malinowski and L. Martinez-Caballero, "A Comparative Study of Three-Phase Inverter Topologies for Common Mode Voltage Reduction in Photovoltaic Applications," 2023 25th European Conference on Power Electronics and Applications (EPE'23 ECCE Europe), Aalborg, Denmark, 2023, pp. 1-8, doi: 10.23919/EPE23ECCEEurope58414.2023.10264522.	Conference	Published	doi: 10.23919/EPE23ECCEEurope58414.2023.10264522.
6	J. Hassan, V. Minambres-Marcos, F. Barrero-Gonzalez and A. A. Alvi, "An Improved Three-Phase Transformerless Neutral Point Clamped Inverter Topology for Common Mode Voltage Reduction," 2023 IEEE 17th International Conference on Compatibility, Power Electronics and Power Engineering (CPE-POWERENG), Tallinn, Estonia, 2023, pp. 1-6, doi: 10.1109/CPE-POWERENG58103.2023.10227487.	Conference	Published	doi: 10.1109/CPE-POWERENG58103.2023.10227487.
7	A. A. Alvi, L. Martínez-Caballero, E. Romero-Cadaval, E. González-Romera, R. Kot and M. Malinowski, "Guidelines for the Application of Genetic Algorithm in Energy Management System," *IECON 2024 - 50th Annual Conference of the IEEE Industrial Electronics Society*, Chicago, IL, USA, 2024, pp. 1-6, doi: 10.1109/IECON55916.2024.10905264.	Conference	Published	doi: 10.1109/IECON55916.2024.10905264.
8	S. M. M. Ahmed *et al.*, "Techno-Economic Optimization of Electric Vehicle Charging Station with Virtual Power Plant – a University Campus Use Case," *IEEE EUROCON 2025 - 21st International Conference on Smart Technologies*, Gdynia, Poland, 2025, pp. 1-6, doi: 10.1109/EUROCON64445.2025.11073409.	Conference	Published	doi: 10.1109/EUROCON64445.2025.11073409.
9	L. Martínez-Caballero, R. Kot, A. Milczarek, M. Malinowski, J. Ding and A. A. Alvi, "Grid Active Power Control with Optimal Battery Usage and Demand Side Management," 2025 IEEE 19th International Conference on Compatibility, Power Electronics and Power Engineering (CPE-POWERENG), Antalya, Turkiye, 2025, pp. 1-6, doi: 10.1109/CPE-POWERENG63314.2025.11027282.	Conference	Published	doi: 10.1109/CPE-POWERENG63314.2025.11027282.

10	A. W. Aslam, A. G. S. Al-Salloomee, A. A. Alvi, F. Barrero-González, V. Minambres-Marcos and C. Roncero-Clemente, "Power Quality Analysis for Selective Harmonic Compensation in Islanded AC Nanogrid," *2025 IEEE 19th International Conference on Compatibility, Power Electronics and Power Engineering (CPE-POWERENG)*, Antalya, Turkiye, 2025, pp. 1-8, doi: 10.1109/CPE-POWERENG63314.2025.11027243.	Conference	Published	doi: 10.1109/CPE-POWERENG63314.2025.11027243.
11	A. A. Alvi, E. Romero-Cadaval, E. González-Romera, M. I. Milanés-Montero, F. Barrero-González and L. Martínez-Caballero, "A Novel Iteration Based Two-Stage Optimization in Energy Management Systems Application For Cost Minimization," *2025 IEEE 19th International Conference on Compatibility, Power Electronics and Power Engineering (CPE-POWERENG)*, Antalya, Turkiye, 2025, pp. 1-6, doi: 10.1109/CPE-POWERENG63314.2025.11027217.	Conference	Published	doi: 10.1109/CPE-POWERENG63314.2025.11027217.
12	González-Romera, E., Roncero-Clemente, C., Romero-Cadaval, E., Milanés-Montero, M. I., Barrero-González, F., & Alvi, A. A. (2025). Two-stage optimization for energy management and power allocation in a Virtual Power Plant of residential microgrids. Renewable Energy and Power Quality Journal, 23(3), 160-165.	Journal	Published	https://doi.org/10.52152/4557
13	Alvi, A.A.; Martínez-Caballero, L.; Romero-Cadaval, E.; González-Romera, E.; Malinowski, M. Iterative Genetic Algorithm to Improve Optimization of a Residential Virtual Power Plant. Energies 2025, 18, 5377. https://doi.org/10.3390/en18205377.	Journal	Published	https://doi.org/10.3390/en18205377

Patents

#	Title	Type (National-Country, International-Scope)	Status (Submitted, published)	REFERENCE

3.4. Task 2.4 – IRP4 "Condition Monitoring for Smart Power Electronic Converter Systems for Distributed Generation"

3.4.1. Introduction

The condition monitoring method included in this deliverable is the work from Aug. 2022 till Oct. 2025, and the research is carried out with the collaboration between Applied Power Electronic Systems (APES) at Aalborg University (the host institute of ESR4) and the Chair of Power Electronics at Kiel University.

The work addresses key challenges in data-driven monitoring, including estimation accuracy, noninvasive online implementation, systematic tool development, and sampling efficiency. Specifically, capacitor health monitoring is improved through joint estimation of capacitance and equivalent series resistance using time-domain voltage measurements and particle swarm optimization. A noninvasive monitoring method for power semiconductor devices is developed by estimating on-state resistance using existing control variables without additional sensors. In addition, a loss-landscape analysis framework is introduced to support systematic design of multi-parameter estimation strategies at the system level. Finally, a switching signal reconstruction method is proposed to improve sampling efficiency by enabling reuse of control-oriented sampling schemes and avoiding costly oversampling. Overall, the results provide low-cost, low-complexity, and accurate condition monitoring approaches that enhance converter reliability and support predictive maintenance in renewable energy systems.

3.4.2. Scientific outcomes

3.1.1.1. Capacitor Condition Monitoring

Background

Capacitors are widely used in power electronic converters for energy storage and voltage ripple mitigation, with electrolytic capacitors commonly adopted due to their high energy density and low cost. During operation, thermal and electrical stresses cause electrolyte evaporation, leading to reduced capacitance (C) and increased equivalent series resistance (ESR). The typical end-of-life criteria are defined as a 20% decrease in capacitance and a 100% increase in ESR. In systems containing many capacitors, such as modular multilevel converters (MMCs) used in HVDC and STATCOM applications, system-level reliability requirements often impose stricter limits on individual capacitor degradation.

Existing capacitor condition monitoring methods can generally be categorized as model-based or data-driven. Model-based approaches typically estimate capacitance using converter electrical characteristics while assuming that ESR has negligible influence. However, this assumption becomes less valid as ESR increases significantly during aging. Data-driven methods have demonstrated the capability to estimate both capacitance and ESR, but often require extensive labeled datasets and computationally intensive algorithms that are difficult to implement on embedded control hardware. Therefore, an important research challenge is to develop a practical monitoring approach that jointly considers the coupling between capacitance and ESR while remaining data-efficient and computationally lightweight for real-time implementation.

System Description

Three-phase MMC with one phase in detail is depicted in Fig. 3.1(a). As demonstrated, three phases are connected with a medium voltage ac grid (v_a, v_b, and v_c) with a filter inductor L_f and a filter resistor R_f, and the grid currents are i_a, i_b, and i_c. Each phase of MMC is composed of two arms, known as the upper and lower arms. A series of connections of submodules with an arm inductor L_{arm} and equivalent arm resistor R_{arm} forms an arm. The topology of the half-bridge submodule is shown in Fig. 3.1(a), which consists of a capacitor and two IGBTs with their antiparallel diode, namely C, S_1, S_2, D_1, and D_2, respectively.

The MMC can be used as an inverter or an active front-end rectifier, where the outer control loop is responsible for it. In a typical MMC controller, the generated current references are considered as inputs of the inner control loop. Then, the reference of the arm voltages is produced and used in the modulation step. Apart from the mentioned controllers, MMC exploits some other controllers to improve the performance of the submodules, such as circulating current control, energy balancing control, etc.

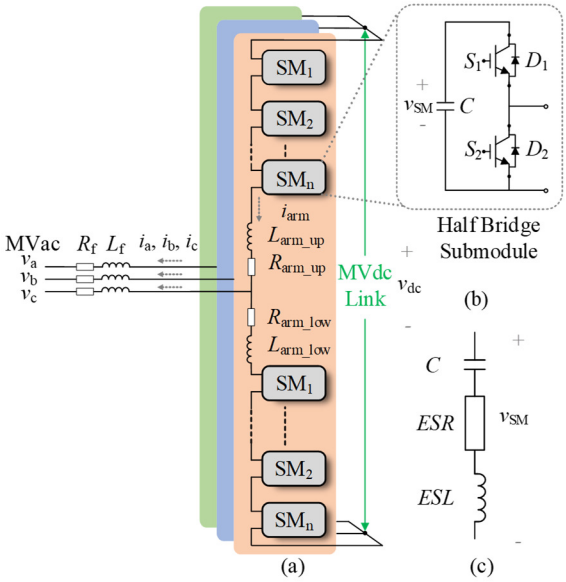

Fig. 3.1. A modular multilevel converter, (a) Converter topology, (b) half-bridge submodule, and (c) model of the submodule capacitor with parasitic parameters.

Proposed Method

To overcome the limitations in the previous capacitor condition monitoring methods, this paper proposes a method to estimate the two health indicators (being capacitance and ESR) together, while not affecting the converter operation.

The system diagram of the proposed method is illustrated in Fig. 3(a). The proposed method starts with taking input signals and initializing capacitance and ESR which are randomly distributed in the solution space. Then the capacitance and ESR are updated with particle swarm optimization, and the updated estimations are used to predict the submodule voltage within a sampling window based on the capacitor voltage equation. The mean square error between the predicted and measured voltage is calculated and compared with an error limit to determine if the update should continue. The condition monitoring method is repeated multiple times (R_m) and the median values of these estimations are taken as the final estimations to avoid using an outlier as the final estimations. The key modules in the flowchart are introduced in the following sections.

Input Signal

Three signals related to one submodule being monitored are measured, including the submodule voltage $v_{SM}(t_k)$, the switching state of the submodule $SW(t_k)$, and the arm current $i_{arm}(t_k)$.

An example waveform is shown in Fig. 3(b). These three signals are time series in a sampling window, $t_k = t_1, t_2, ..., t_N$. The sampling window is selected as half of the fundamental cycle within which there are some switching transients because it is important for ESR estimation [23], while the window is shorter than a fundamental cycle to mitigate the error in the voltage prediction process. The sampling frequency is 100 kHz, which is much higher than the switching frequency of an MMC (usually lower than several kHz [30]) to ensure the prediction accuracy.

Update C and ESR with Particle Swarm Optimization

Particle swarm optimization (PSO) is a classical metaheuristic search method. It searches the solution space with a group of particles and the positions of the particles are updated gradually with shared information to find the optimal solution. In the proposed method, each particle has a 2-dimensional position: estimated capacitance and ESR. The position of each particle leads to an individual voltage error, and the position with the lowest error is the optimal position. In the initialization stage, each particle is assigned with a random position within the solution space and a random velocity. In each iteration, particles update their velocities and positions according to their own position, individual optimal position, and the global optimal position [31]:

$$v_j = \omega_j v_{j-1} + c_1 r_{1j}(x_p - x_{j-1}) + c_2 r_{2j}(x_g - x_{j-1})$$
$$x_j = x_{j-1} + v_j \quad (1)$$

where v_j and v_{j-1} are velocities, x_j and x_{j-1} are positions of the current j^{th} iteration and the last $(j-1)^{th}$ iteration, respectively; x_p and x_g are individual and global optimal positions; ω_i, c_1, and c_2 are inertia weight, cognitive weight

and social weight, respectively; r_{1j} and r_{2j} are two random numbers between 0 and 1, varying in each iteration. The inertia weight ω_j decreases gradually so that as the iteration increases, the velocity reduces and the searching step becomes more refined [31]. The reducing velocity can be seen on the trajectory, which moves in a wider range at the beginning and becomes more stable at the end in Fig. 3(c) wherein three simplified trajectories are plotted as green dashed lines.

Eq. 1 shows that the positions are updated according to the global and individual optimal solution, so the voltage errors of all particles reduce gradually, and the positions of particles move to the optimal solution gradually. In other words, the update process uses particles to approach the actual values.

Voltage Prediction and Error Calculation

The voltage prediction block takes the measured signals (i.e., $i_{arm}(t_k)$ and $SW_1(t_k)$) as well as the estimated parameters (i.e., and C) to predict a series of submodule voltage $_{SM}(t_k)$, where $t_k = t_1, t_2, ..., t_N$ covering the entire sampling window. At the first time step t_1, $_{SM}(t_1) = v_{SM}(t_1)$. After t_1, the prediction starts from the second time step t_2 to the last time step t_N in the sampling window, and the prediction is based on a capacitor voltage equation:

The submodule voltage error is compared with an error limit to determine if the capacitance and ESR estimations should be updated. A large error indicates that the estimations deviate significantly from the actual value while a small error reveals that the estimations are close to the actual values. Fig.3(d) shows the voltage prediction waveforms. When the estimated capacitance and ESR are different from 1 p.u., the prediction waveforms in dashed lines significantly deviate from the measured voltage (a solid blue line). The voltage error against the normalized capacitance and ESR when their counterparts are 1 p.u. are given in Fig. 3(e), which shows that the voltage error is minimized when both estimations achieve 1 p.u.

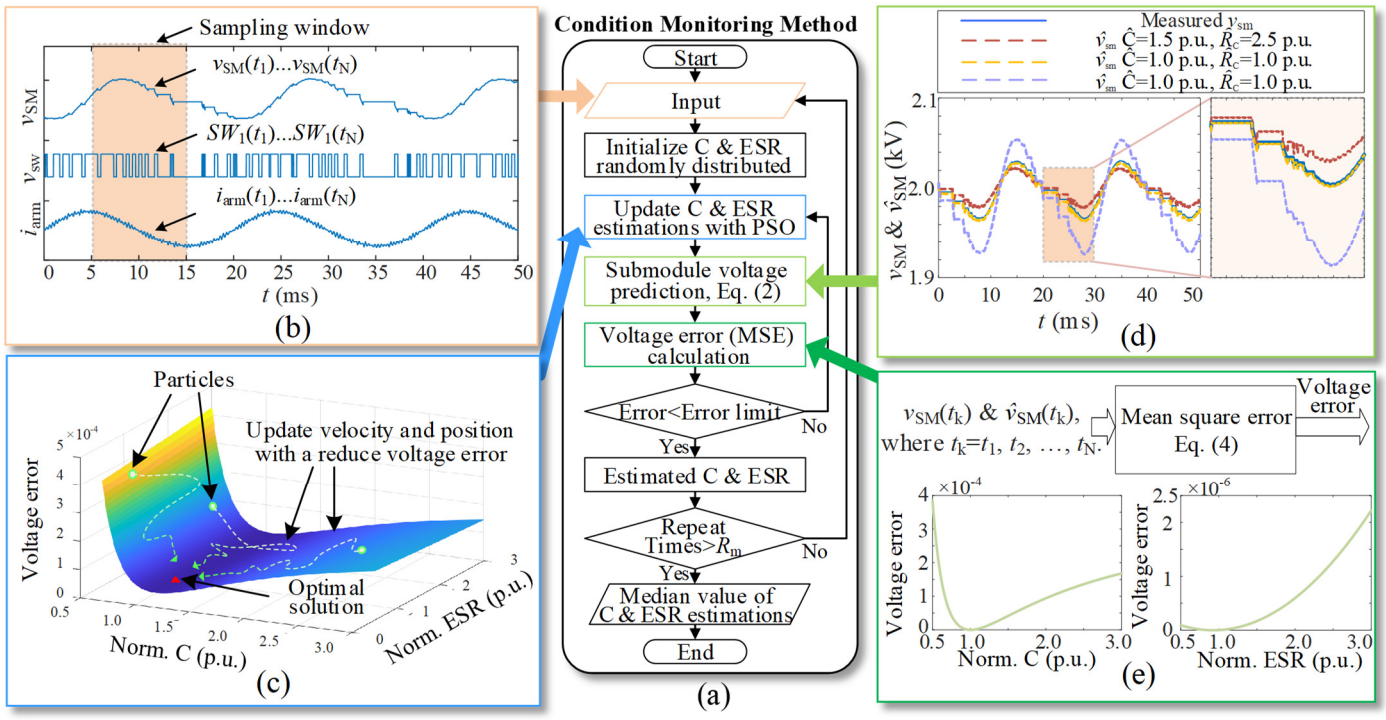

Fig. 3.2 A system diagram of the proposed condition monitoring method: (a) a flowchart of the condition monitoring method; (b) a sampling window of three input signals: the submodule voltage $v_{SM}(t_k)$, the switching state $SW_1(t_k)$, and the arm current $i_{arm}(t_k)$, where time $t_k = t_1, t_2, ..., t_N$ consists of N time steps; (c) the particle swarm optimization (PSO) method updates the positions of each particle to have a low voltage error; (d) the voltage prediction module predicts the submodule voltage $_{SM}(t_k)$ in the sampling window, where the prediction with 1 p.u. estimations is closer to the measured voltage; (e) the mean square error between predicted and measured voltage error is calculated, and it is minimized when both C and ESR are 1 p.u.

Validation

The estimation waveforms and results are illustrated in Fig. 3.3 and Table 3.1, with around 1% and 10% estimation errors for the capacitance and ESR.

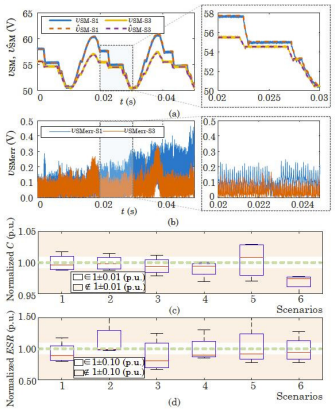

Fig. 3.3: Evaluation of submodule voltage prediction and health indicator estimation accuracy. (a) Time-domain waveforms of measured and estimated submodule voltages under Scenarios 1 and 3 over 2.5 cycles; (b) Instantaneous voltage error between measured and predicted values; (c) Boxplots of capacitance estimations; (d) Boxplots of ESR estimations.

Scenario	1	2	3	4	5	6
V_{SMDC} (V)	50 V			30 V		
$I^{\star}_{AC}$ (A)	9	6	3	9	6	3
C_{err} (%)	0.35	0.18	0.66	0.57	0.83	2.56
ESR_{err} (%)	11.47	0.41	19.73	9.71	8.68	5.90

Table 3.1: Mission profile emulator experimental conditions and estimation results.

Conclusion

This part presents a particle swarm optimization (PSO)–based method for condition monitoring of aluminum electrolytic capacitors in modular multilevel converters (MMCs) by jointly estimating capacitance (C) and equivalent series resistance (ESR). Unlike conventional approaches that rely on a single health indicator, the proposed method captures the coupled degradation behavior of both parameters and does not assume ESR to be negligible, maintaining estimation accuracy even as ESR increases. The approach is validated using a mission-profile emulator, and is implemented on a DSP platform to demonstrate feasibility for edge-based monitoring. Experimental results show estimation errors mostly below 1% for capacitance and 10% for ESR.

3.1.1.2. Switching Device Condition Monitoring

Background

Power semiconductor devices are key components in power electronic converters and are subjected to significant thermal and electrical stresses during operation. Thermal cycling causes mechanical strain in the multi-layer packaging structure due to mismatched thermal expansion coefficients, leading to degradation mechanisms such as bond wire cracking or lift-off, particularly in insulated-gate bipolar transistors (IGBTs). These degradation processes typically result in increased on-state resistance or eventual open-circuit failure. Various health indicators have been proposed to monitor such degradation, including on-state voltage, turn-on voltage overshoot, short-circuit current, magnetic field, and differential-mode interference. Among them, on-state voltage is the most widely used indicator due to its high sensitivity and suitability for online monitoring.

However, direct measurement of on-state voltage usually requires additional sensing circuits with high bandwidth, high resolution, and strong noise immunity, which increases system complexity, cost, and potential reliability risks in practical applications. To address these limitations, noninvasive monitoring approaches have been explored, such as estimating device degradation through deviations in control variables caused by changes in on-state voltage. Although promising, these data-driven approaches often rely on large training datasets that capture both device degradation and converter operating conditions, making their practical deployment challenging. Consequently, there is a need for monitoring methods that enable reliable online condition assessment while avoiding invasive hardware modifications and extensive training data requirements.

System Description

The proposed method is implemented on a three-phase inverter system widely used in renewable energy applications. The inverter employs an IGBT module consisting of six switches with corresponding free-wheeling diodes, a DC-link capacitor to maintain the DC voltage, and a grid interface through an inductor filter and series

resistance. The converter is controlled in the synchronous *dq*-reference frame, where the measured phase currents are transformed into i_d and i_q components and regulated using proportional–integral controllers. The resulting voltage references are combined with grid-voltage feed-forward terms to improve dynamic performance, transformed back to the stationary frame, and applied to a pulse-width modulation unit to generate the switching gate signals, with the coordinate transformation synchronized by a phase-locked loop estimating the grid voltage phase angle.

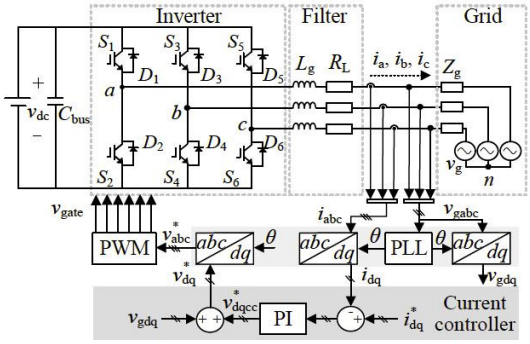

Fig. 3.4: Configuration of a three-phase inverter along with its control strategy in the synchronous reference frame, in which PWM refers to pulse-width modulation; PI denotes the proportional-integral regulator; abc is the stationary frame and dq is the synchronous frame; and PLL denotes the phase-locked loop.

Proposed Method

To achieve noninvasive monitoring without additional hardware, the equivalent on-state current and voltage of IGBT S_1 are estimated using existing control variables and measurements, including the current controller output $v^*_a(t)$, inverter current $i_a(t)$, grid voltage $v_{ga}(t)$, and DC-link voltage $v_{dc}(t)$. The IGBT current is derived from the phase current under positive conduction using the modulation signal, which replaces the gate signal to avoid high-speed sensing requirements. The on-state voltage variation is then inferred from deviations in the current controller output that compensate for the device voltage drop. By combining the estimated current and voltage signals, the on-state resistance can be evaluated, while additional processing is required to mitigate estimation errors caused by measurement noise.

To reduce noise and obtain stable resistance estimation, an accumulation and averaging process is applied. The instantaneous current and voltage signals are first accumulated over one fundamental cycle using switching-cycle sampling, producing accumulated current and voltage values. These quantities are then averaged over a longer sampling window (e.g., 200 s) across repeated operating points in the mission profile, which improves robustness against measurement noise while maintaining compatibility with typical converter operation. Finally, the increase in on-state resistance is calculated using Ohm's law based on the change in the control-variable voltage and the corresponding accumulated current, with a scaling factor applied to account for coordinate transformation in the control system.

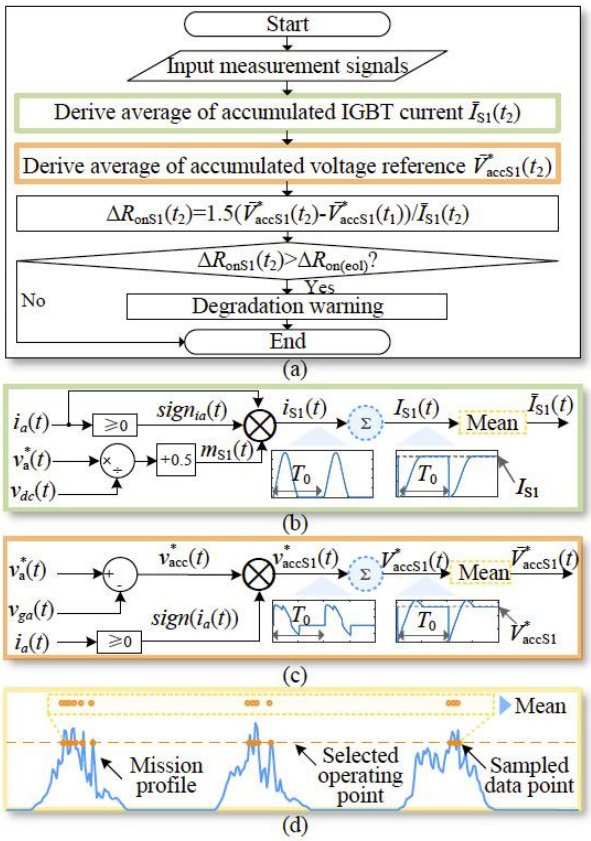

Fig. 3.5: Flowchart and key steps for the proposed monitoring strategy: (a) Overall procedure of the method. (b) Derivation of the equivalent current $I_{S1}(t)$ flowing through S_1. (c) Derivation of the equivalent voltage $V^*_{accS1}(t)$. (d) Computation of the increase in on-state resistance ΔR_{on} using multiple samples at the selected operating point.

Validation

As illustrated in Fig. 3.6, the proposed condition monitoring method is evaluated under three scenarios that may affect estimation performance: varying on-state resistance of switch S_1, different inverter power levels, and varying power factors. The IGBT parameters follow the Infineon FS50R12KT4 module, with an initial on-state resistance of 25 mΩ and an end-of-life threshold defined by a 2 mΩ increase. Under varying resistance conditions, the estimated values closely follow the actual resistance with an average error of 0.29 mΩ (1.16%), well below the end-of-life threshold. Additional tests under different power levels (5–20 kW) and power factors show estimation errors of 0.27 mΩ (1.08%) and 0.17 mΩ (0.68%), respectively. These results demonstrate that the proposed method achieves high estimation accuracy and remains robust under varying operating conditions.

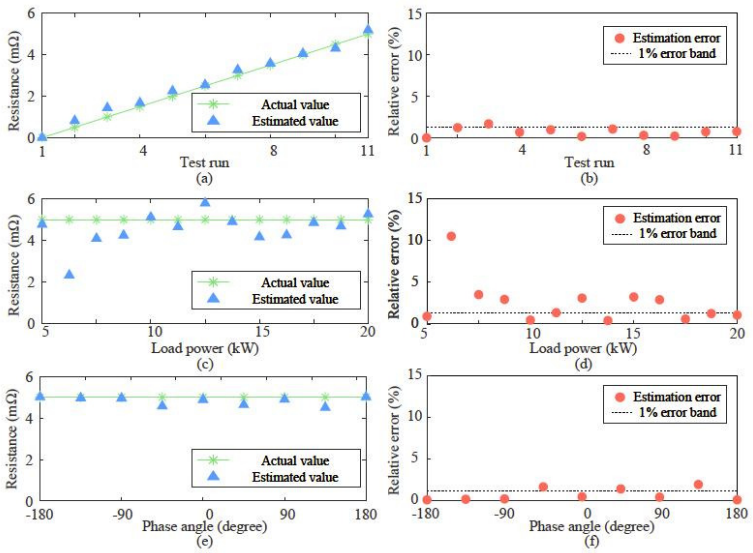

Fig. 3.6: HIL validation under varying conditions: (a) Estimations compared with the increasing on-state resistance (Case I). (b) Estimation errors in Case I. (c) Estimations at different power levels (Case II). (d) Estimation errors in Case II. (e) Estimations at varying power factors (Case III). (f) Estimation errors in Case III.

Conclusion

The proposed on-state voltage estimation approach enables noninvasive online monitoring by relying solely on existing control variables and measurement signals, eliminating the need for additional sensors and preserving converter cost and hardware complexity. Compared with other noninvasive solutions, the method offers broader applicability across different system configurations and incorporates a noise mitigation strategy to improve robustness. Hardware-in-the-loop testing under three scenarios shows that output power has a stronger influence on estimation accuracy than resistance variation or power factor. The method achieves its highest accuracy under full-load conditions, with an average estimation error below 2% of the initial resistance.

3.1.1.3. Buck Converter Condition Monitoring

Background

To extend condition monitoring from individual components to multiple devices, increasing attention has been directed toward system-level monitoring approaches. These methods evaluate the health status of several components within power converters using measurements already available for control purposes, such as output voltage and inductor current. They are often studied on basic converter topologies, such as buck converters, whose relatively simple structures facilitate analysis and algorithm development.

System-level monitoring methods can generally be categorized into non-circuit-parameter and circuit-parameter estimation approaches. Non-circuit-parameter methods detect degradation through changes in transfer functions or statistical deviations in system states, but the relationship between these variations and specific component degradation is often ambiguous. In contrast, circuit-parameter-based methods estimate physical parameters directly associated with component health, enabling clearer diagnosis of degradation mechanisms. These methods typically formulate monitoring as a time-domain regression problem, where a converter state-space model predicts electrical signals, the prediction error is evaluated, and optimization algorithms update the estimated circuit parameters.

Despite their advantages, existing circuit-parameter-based approaches still face important challenges. Different parameters exhibit inconsistent estimation accuracy and variability, yet the underlying reasons for these differences remain insufficiently understood. In addition, most existing methods rely on oversampling electrical signals, often several times higher than the switching frequency, which imposes significant demands on sensing hardware, communication bandwidth, and computational resources. Therefore, improved methods are needed to systematically assess multi-parameter estimation performance and develop more efficient sampling strategies compatible with practical control-oriented measurement schemes.

System Description

The system-level condition monitoring method is demonstrated using a buck converter consisting of an inductor, an electrolytic capacitor, a MOSFET, a diode, and a resistive load. Key non-ideal characteristics are included, such as the equivalent series resistances of the inductor and capacitor, the MOSFET on-state resistance, and the diode forward voltage. The converter operates under cascaded voltage–current control, where the output voltage and inductor current are regulated by adjusting the switching duty cycle. The monitoring method uses the state-vector signals i_L and v_O collected during a load transient, which provides strong excitation for parameter estimation while limiting data size. The analysis assumes continuous-conduction mode operation, as discontinuous-conduction mode would require additional modeling complexity.

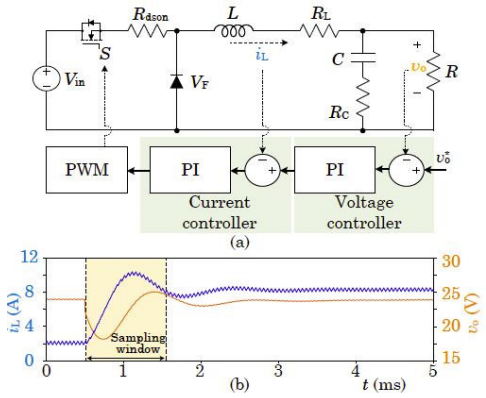

Fig. 3.7: Buck converter system and representative waveforms: (a) Buck converter and control system, in which PWM represents the pulse-width modulation and PI denotes the proportional-integral regulator. (b) Input signals are captured during a load step, including an inductor current and an output voltage.

Proposed Method for Performance Evaluation

The general methods are introduced in Fig. 3.8, in which the circuit parameters affect the loss values. By changing the circuit parameters around their actual values, a loss landscape can be derived as illustrated in Fig. 3.9.

Loss landscape analysis examines the geometric properties of the objective function in parameter space to understand how parameter variations affect optimization convergence and estimation accuracy. In system-level condition monitoring, the loss function depends on the estimated circuit parameters θ_0={L, C, R, R_C, R_L, R_{dson}, V_F}. By analyzing the loss landscape, it becomes possible to interpret the optimization behavior and estimation performance of different parameters.

Results show that parameters with larger loss magnitudes and smoother loss curves, such as L, C, R, R_C, are easier to estimate accurately and consistently. In contrast, parameters such as R_L, R_{dson}, and V_F exhibit smaller loss magnitudes and more oscillatory loss curves, leading to slower convergence, higher estimation variability, and potential local optima. This analysis explains differences in estimation performance across parameters and provides insight for designing more reliable multi-parameter condition monitoring strategies.

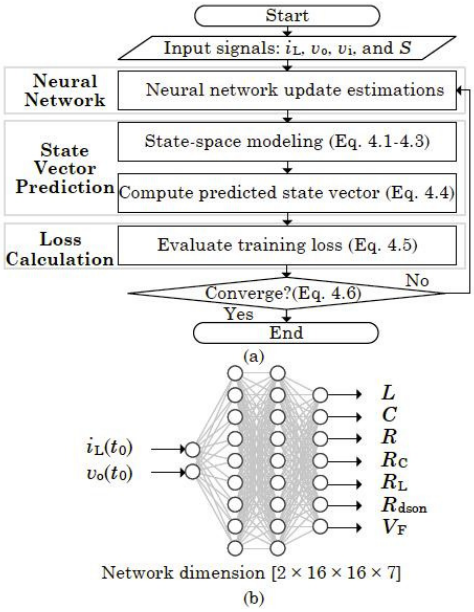

Fig. 3.8: System-level condition monitoring with time-domain regression: (a) The general flowchart including optimization, state-vector prediction, and loss calculation. (b) The architecture of the neural network.

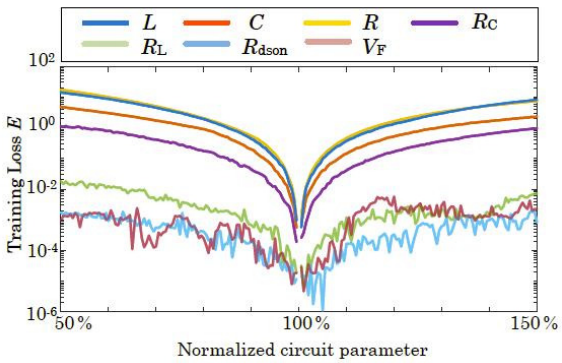

Fig. 3.9: The example loss landscape of the circuit parameters in the buck converter.

Validation

The converter is evaluated under three load-step conditions to study their impact on parameter estimation. The load increases from 50 W to different levels: 200 W (Case 1), 150 W (Case 2), and 100 W (Case 3). Results show that larger load steps produce smoother loss curves and improve convergence of parameter estimation. Parameters such as C

and R_C exhibit higher loss magnitudes and smoother landscapes, leading to more stable and accurate estimation compared with parameters like R_{dson}.

Validation using ten independent runs confirms these observations. The parameter subset θ_1={L, C, R, R_C} achieves high accuracy and consistency, with median errors below 3%. In contrast, parameters θ_2={R_L, R_{dson}, V_F} show significantly larger errors and variability, indicating difficulty in achieving reliable convergence.

Additional tests evaluate robustness against measurement noise by introducing Gaussian noise at levels from 5 to 50 times the ADC resolution. Increasing noise makes the loss landscape flatter and more oscillatory, leading to larger estimation errors. Nevertheless, parameters in θ_1 remain relatively robust with errors below 11%, while parameters in θ_2 exhibit strong sensitivity to noise and reduced estimation stability.

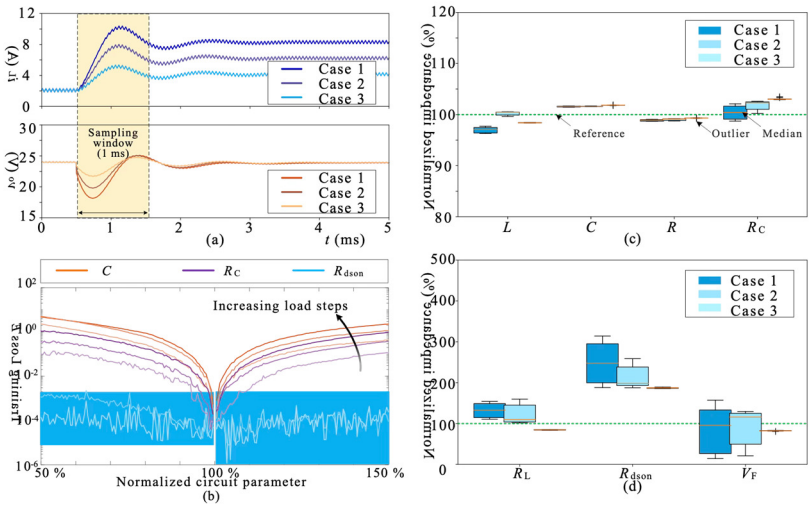

Fig. 3.10 (a) Waveforms and estimations of three load steps. (b) Loss landscape. (c-d) Estimated circuit parameters θ_1 and θ_2.

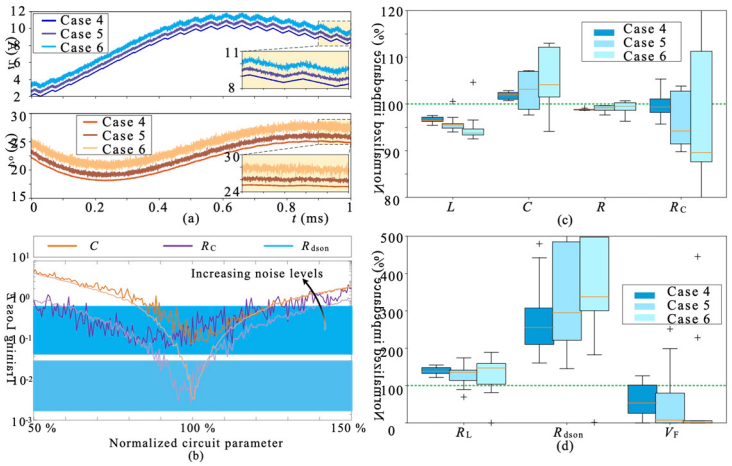

Fig. 3.11 (a) Waveforms and estimations of three load steps. (b) Loss landscape. (c-d) Estimated circuit parameters θ_1 and θ_2.

Conclusion

Time-domain regression–based system-level condition monitoring methods are assessed using loss landscape analysis. Results show that only a subset of circuit parameters, primarily L, C, and R, can meet estimation accuracy requirements, with L and C being the most suitable indicators for condition monitoring due to their strong relation to component degradation.

The analysis unifies existing approaches into a general framework consisting of prediction, loss calculation, and optimization. By examining the magnitude and smoothness of the loss curves, circuit parameters can be classified into three categories: accurately estimated, condition-dependent, and unreliably estimated parameters. Simulation results confirm that parameters L, C, and R exhibit high accuracy and stability, while others are more sensitive to operating conditions and contribute less to the objective function.

Overall, loss landscape analysis provides a practical framework for understanding differences in multi-parameter estimation performance and guiding the design of condition monitoring strategies. It also highlights limitations of current approaches and identifies potential directions for improving parameter estimation in more complex systems.

3.4.3. Contribution to the WP objectives

The work in this deliverable contributes to the work package objective of improving reliability and reducing waste in renewable energy generation systems through the development of advanced condition monitoring methods for power electronic converters. Since converters are critical interfaces in renewable energy systems, early detection of component degradation enables predictive maintenance and prevents unexpected failures, thereby extending component lifetime and reducing unnecessary replacement.

Three levels of monitoring solutions are developed. First, a PSO-based capacitor condition monitoring method jointly estimates capacitance and ESR, capturing their coupled degradation behavior and enabling accurate health assessment of electrolytic capacitors, which are among the most failure-prone components in converters. Second, a noninvasive monitoring approach for switching devices estimates the on-state resistance of power semiconductors using existing control variables, eliminating the need for additional sensors while enabling online detection of device degradation. Third, a system-level condition monitoring framework evaluates the feasibility of estimating multiple circuit parameters using loss landscape analysis, identifying which parameters can be reliably monitored and guiding the design of robust monitoring strategies.

Together, these contributions provide low-cost, noninvasive, and data-efficient monitoring solutions that support reliable operation of power converters in renewable energy applications. By enabling early fault detection, improving diagnostic accuracy, and facilitating predictive maintenance, the proposed methods help extend equipment lifetime, reduce downtime, and minimize material waste associated with premature component replacement, thereby directly supporting the goals of the work package.

3.4.4. Scientific achievements

Experimental prototypes

#	Name	Description	Status (designed, assembled, tested)	Photo
1	Mission-profile emulator	A modular test platform to simplify the MMC capacitor reliability test by reproducing the similar operating waveform and stress level on the submodule capacitor.	Tested	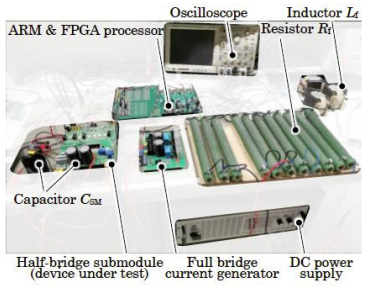
2	Hardware-in-the-loop (HIL) switching device test setup	Using HIL test setup to emulate different health status of the switching devices.	Tested	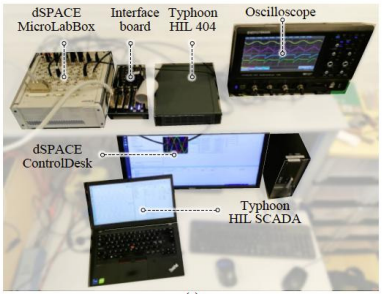

3	Buck converter test setup	Using the buck converter test setup to collect operating waveforms, enabling converter parameter estimation.	Tested	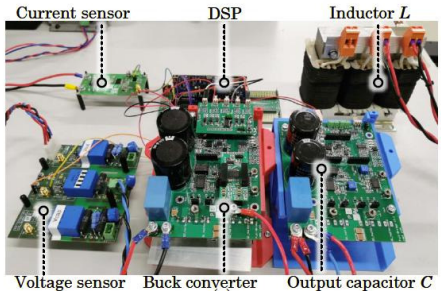

Publication

#	Title, incl. citation information	Type (Conference, journal, book chapter)	Status (Submitted, accepted, published)	DOI
1	Monolithic Data-Driven Condition Monitoring Strategy for MMC Considering C and ESR	Journal	Accepted	10.1109/TPEL.2025.3549226
2	Data-Light Oscillation Mode Identification for Fast Stability Assessment of Grid Tied Converters	Journal	Accepted	10.1109/TPEL.2025.3556387
3	A Low-Sampling Frequency Condition Monitoring Method for Buck Converter	Journal	Submitted	NA
4	A Data-Driven Condition Monitoring Method for Capacitor in Modular Multilevel Converter (MMC)	Conference	Accepted	10.1109/IPEMC-ECCEAsia60879.2024.10567101
5	Semiconductor Devices Condition Monitoring Using Harmonics in Inverter Control Variables	Conference	Accepted	10.23919/EPE23ECCEEurope58414.2023.10264538
6	A Sensorless IGBT On-State Voltage Estimation Method Using Inverter Control Variable	Conference	Accepted	10.1109/APEC48143.2025.10977401
7	Physics-Informed Neural Network for Parameter Identification: a Buck Converter Case Study	Conference	Accepted	10.1109/ECCE-Asia63110.2025.11111770

4. Conclusions

This deliverable presents the final scientific outcomes of Work Package 2 (WP2) within the SMARTGYsum project, focusing on green, renewable distributed electric energy generation and storage. The work carried out across IRP1–IRP4 has addressed key challenges in reliability, efficiency, power quality, and the coordinated operation of distributed energy resources. The results demonstrate the importance of advanced inverter-based systems and control strategies in improving reliability, power quality, and coordinated operation of distributed generation. In IRP1, cooperative smart-inverter technologies were developed and validated, including hybrid inverter architectures, decentralized control strategies, and power-quality enhancement techniques suitable for residential nanogrids. IRP2 contributed to the design and experimental validation of power generators for smart buildings, including advanced control methods and energy management strategies enabling reliable and flexible operation. IRP3 introduced a Virtual Power Plant framework with optimization algorithms and a digital twin, enabling coordinated operation of distributed resources to achieve both technical and economic objectives. IRP4 focused on condition-monitoring methods for power electronic converters, improving system reliability through advanced diagnostics.
Across all IRPs, the integration of simulation, Hardware-in-the-Loop validation, and experimental prototypes ensured the practical relevance and applicability of the proposed solutions. The results confirm that distributed renewable energy systems can be effectively coordinated while maintaining stability, power quality, and operational efficiency, even under non-linear and dynamic conditions.

Collaboration among ESRs and partner institutions was effective and contributed significantly to the quality of the outcomes. The ESRs demonstrated strong technical competence, adaptability, and the ability to work across disciplines and institutions, which was reflected in joint activities, secondments, and co-authored publications. The training provided to ESRs has significantly contributed to their professional development.
In addition to the technical contributions, WP2 has achieved strong dissemination outcomes, including conference and journal publications, as well as active participation in doctoral schools and secondments.

Overall, WP2 has successfully met its objectives and provided a coherent set of technological and methodological advancements supporting the transition towards smart, reliable, and sustainable energy systems. The outcomes establish a solid foundation for future research, development, and deployment of distributed renewable energy solutions within smart grids and energy communities.

5. References

1. A. W. Aslam, J. Hassan, V. Minambres-Marcos, A. G. S. Al-salloomee, and C. Roncero-Clemente, "Traditional and hybrid topologies for single-/three-phase transformerless multilevel inverters," Electronics, vol. 13, no. 20, art. 4058, 2024, doi: 10.3390/electronics13204058.
2. A. W. Aslam, A. G. S. Al-Salloomee, J. Gutiérrez-Escalona, C. Roncero-Clemente, and V. Minambres-Marcos, "Tuning and assessment of inner control loops in an islanded nanogrid with harmonic and unbalanced loads," in Proc. 2025 Int. Aegean Conf. Elect. Mach. Power Electron. (ACEMP) & 2025 Int. Conf. Optim. Electr. Electron. Equip. (OPTIM), 2025, pp. 1–6, doi: 10.1109/OPTIM-ACEMP62776.2025.11075248.
3. A. W. Aslam, A. G. S. Al-Salloomee, A. A. Alvi, F. Barrero-González, V. Minambres-Marcos, and C. Roncero-Clemente, "Power quality analysis for selective harmonic compensation in islanded AC nanogrid," in Proc. 2025 IEEE 19th Int. Conf. Compatibility, Power Electron. Power Eng. (CPE-POWERENG), 2025, pp. 1–6, doi: 10.1109/CPE-POWERENG63314.2025.11027243.
4. A. W. Aslam, V. Minambres-Marcos, and C. Roncero-Clemente, "A residential droop-controlled AC nanogrid with power quality enhancement," Electronics, vol. 14, no. 16, art. 3306, 2025, doi: 10.3390/electronics14163306.
5. L. Martínez-Caballero, A. Aslam, R. Kot, A. Milczarek, and M. Malinowski, "A control strategy for a standalone PV-battery system operating at SoC boundaries with DC-link ripple management," IEEE Access, vol. 13, pp. 123456–123469 (final pages as per journal), 2025, doi: 10.1109/ACCESS.2025.3625405.
6. A. W. Aslam and V. Minambres-Marcos, "Business model development for a hybrid AC nanogrid with parallel inverter topology: Integrating engineering and economic perspectives," J. Mod. Power Syst. Clean Energy, submitted for publication, 2025 (DOI pending).
[J1] S. Ou, M. Hassanifar, M. Votava, A. Sangwongwanich, S. Sahoo, M. Langwasser, M. Liserre, F. Blaabjerg, "Monolithic Data-Driven Condition Monitoring Strategy for MMC Considering C and ESR", *IEEE Trans. Power Electron.*, vol. 40, no. 8, pp. 11339-11354, Aug. 2025.

[J2] S. Ou, S. Sahoo, A. Sangwongwanich, M. Langwasser, M. Hassanifar, M. Votava, M. Liserre, F. Blaabjerg, "A Low-Sampling Frequency Condition Monitoring Method for Buck Converter", submitted to *IEEE J. Emerg. Sel. Top. Ind. Electron.,* under review.
[J3] R. Kong, S. Sahoo, S. Ou, X. Meng, G. Gao and F. Blaabjerg, "Data-Light Oscillation Mode Identification for Fast Stability Assessment of Grid-Tied Converters," *IEEE Trans. Power Electron.*, vol. 40, no. 8, pp. 11170-11181, Aug. 2025.
[C1] S. Ou, M. Hassanifar, M. Votava, A. Sangwongwanich, S. Sahoo, M. Langwasser, M. Liserre, F. Blaabjerg, "A Data-Driven Condition Monitoring Method for Capacitor in Modular Multilevel Converter (MMC)", in *Proc. IPEMC-ECCE Asia, Chengdu,* China, May 2024, pp. 4528-4535.
[C2] S. Ou, A. Sangwongwanich, S. Sahoo, F. Blaabjerg, "Semiconductor Devices Condition Monitoring Using Harmonics in Inverter Control Variables", in *Proc. EPE'23 ECCE Europe*, Aalborg, Denmark, Sept. 2023, pp.1-8.
[C3] S. Ou, S. Sahoo, A. Sangwongwanich, Y. Liu, F. Blaabjerg, "A Sensorless IGBT On-State Voltage Estimation Method Using Inverter Control Variables", in *Proc. 2025 APEC*, GA, USA, Mar. 2025, pp.1501-1506.
[C4] S. Ou, S. Sahoo, A. Sangwongwanich, F. Blaabjerg, M. Hassanifar, M. Votava, M. Langwasser, M. Liserre, "Physics-Informed Neural Network for Parameter Identification: a Buck Converter Case Study", in *Proc. IPEMC2025-ECCE Asia*, Bangaluru, India, May. 2025, pp.1-6.
[1] L. Martínez-Caballero, A. Wajiha Aslam, R. Kot, A. Milczarek, and M. Malinowski, "A Control Strategy for a Standalone PV-Battery System Operating at SoC Boundaries With DC-Link Ripple Management," *IEEE Access*, vol. 13, pp. 183706–183721, 2025, doi: 10.1109/ACCESS.2025.3625405.
[2] L. Martínez-Caballero, R. Kot, A. Milczarek, and M. Malinowski, "Comparison of Energy Storage Management Techniques for a Grid-Connected PV- and Battery-Supplied Residential System," *Electronics*, vol. 13, no. 1, Art. no. 1, Jan. 2024, doi: 10.3390/electronics13010087.
[3] L. Martínez-Caballero, R. Kot, A. Milczarek, and M. Malinowski, "Converter Averaging Approach for Modeling a Residential Supply Subsystem," in *2023 IEEE 17th International Conference on Compatibility, Power Electronics and Power Engineering (CPE-POWERENG)*, Jun. 2023, pp. 1–6. doi: 10.1109/CPE-POWERENG58103.2023.10227486.
[4] A. Milczarek and L. Martinez-Caballero, "Control Strategy of Hybrid Energy Storage System for High-Dynamic Load Changes," in *2023 IEEE 17th International Conference on Compatibility, Power Electronics and Power Engineering (CPE-POWERENG)*, Jun. 2023, pp. 1–5. doi: 10.1109/CPE-POWERENG58103.2023.10227479.
[5] L. Martínez-Caballero, R. Kot, A. Milczarek, and M. Malinowski, "A Current Control Method for an Interleaved Boost Converter Under CCM/DCM Operation in a PV System," in *2024 IEEE 18th International Conference on Compatibility, Power Electronics and Power Engineering (CPE-POWERENG)*, Jun. 2024, pp. 1–6. doi: 10.1109/CPE-POWERENG60842.2024.10604371.
[6] L. Martínez-Caballero, R. Kot, A. Milczarek, and M. Malinowski, "Soft-Start Method for Boost Converter Under Rapid Irradiance Changes," in *IECON 2024 - 50th Annual Conference of the IEEE Industrial Electronics Society*, Nov. 2024, pp. 1–6. doi: 10.1109/IECON55916.2024.10905290.
[7] A. Milczarek, R. Kot, L. Martínez-Caballero, and M. Malinowski, "An Intentional Islanded Mode of Operation for a Four-Leg Converter Under Rapid and Asymmetrical Load Changes," in *IECON 2024 - 50th Annual Conference of the IEEE Industrial Electronics Society*, Nov. 2024, pp. 1–7. doi: 10.1109/IECON55916.2024.10905463
[8] L. Martínez-Caballero, R. Kot, A. Milczarek, M. Malinowski, J. Ding, and A. A. Alvi, "Grid Active Power Control with Optimal Battery Usage and Demand Side Management," in *2025 IEEE 19th International Conference on Compatibility, Power Electronics and Power Engineering (CPE-POWERENG)*, May 2025, pp. 1–6. doi: 10.1109/CPE-POWERENG63314.2025.11027282.